



FACILITY FORM 602

**N66-10616**

(ACCESSION NUMBER)

(THRU)

(PAGES)

(CODE)

(NASA CR OR TMX OR AD NUMBER)

(CATEGORY)

20023-FR1-A

FINAL REPORT

**GG159 MINIATURE INTEGRATING GYRO  
STERILIZATION EXPOSURE STUDIES AT 300°F**

**California Institute of Technology  
Jet Propulsion Laboratory  
Pasadena, California**

JPL Contract No. 950769

10 September 1965

**HONEYWELL**

*Aeronautical Division*

GPO PRICE \$ \_\_\_\_\_

CFSTI PRICE(S) \$ \_\_\_\_\_

Hard copy (HC) 3.00

Microfiche (MF) 75

10 September 1965

FINAL REPORT

GG159 MINIATURE INTEGRATING GYRO  
STERILIZATION EXPOSURE STUDIES AT 300°F

California Institute of Technology  
Jet Propulsion Laboratory  
Pasadena, California

JPL Contract No. 950769

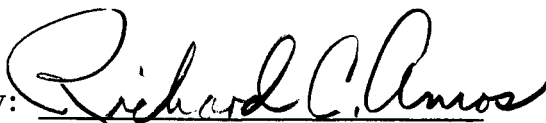
*under NAS 7-100*

Prepared and Approved by:



R. G. Baldwin  
Project Engineer  
Inertial Components

Reviewed by:



Richard C. Amos  
Program Administrator  
Program Management



M. H. Riesgraf  
Section Head  
Inertial Components

Honeywell Inc.  
Aeronautical Division  
Minneapolis, Minnesota

## CONTENTS

	Page
SECTION I INTRODUCTION	1
SECTION II PHYSICAL DESCRIPTION OF THE GG159 GYRO	2
SECTION III SUMMARY	7
Materials Study and Gyro Development	7
Materials Study	7
Gyro Development	8
Spinmotor Failure and Corrective Action	9
Final Gyro Performance	9
Drift Stability and Random Drift	10
G <sup>2</sup> Drift Coefficients	10
Spinmotor Runup-to-Runup Stability	10
Null Repeatability and Elastic Restraint	10
SECTION IV MATERIALS STUDY	13
Gimbal Flotation Fluid	13
Physical Specifications	14
Corrosion Tests	15
Fluid Stability	18
Conclusions	19
Adhesives	20
Test Procedures	20
Conclusions	22
O-Rings	22
Test Procedures	23
Conclusions	23
Balance Ring	25
Eutectic Alloy, Balance Pan	25
Gyro Case Material	26
Test Procedure	26
Conclusions	28
Wire Insulations	28
Conclusions	28

CONTENTS

		Page
SECTION V	GYRO DEVELOPMENT	29
	Gimbal Flotation	29
	Pump Assembly	30
	Hysteresis Ring	33
SECTION VI	EXPERIMENTAL GYRO	35
	Gyro Description	35
	Conclusions	38
SECTION VII	INITIAL GYRO PERFORMANCE	40
	Calibration and Adjustments	40
	Test Results	41
	G <sup>2</sup> -Drift	41
	Reference Drift Rate	41
	Drift Rate Shift	41
	Spinmotor Runup-to-Runup Stability	43
	Random Drift	43
	Gyro Parameters	43
	Discussion and Conclusions	44
SECTION VIII	SPINMOTOR FAILURE ANALYSIS AND CORRECTIVE ACTION	45
	Preliminary Failure Analysis	45
	Failure Analysis	46
	Corrective Action	51
	Gyro Re-Build and Pump Failure	54
	Discussion and Conclusions	55
SECTION IX	FINAL GYRO PERFORMANCE	56
	Calibration and Adjustments	56
	Test Results	56
	G <sup>2</sup> Drift	56
	Reference Drift Rate	58
	Drift Rate Shift	58
	Spinmotor Runup-to-Runup Stability	59
	Random Drift	59
	Gyro Parameters	60
	Six-Position Test Results	60
	Spinmotor Performance	65
	Starting Characteristics	65
	Synchronous Characteristics	65
	Conclusions	66
SECTION X	RECOMMENDATIONS	68
	Magnetic	68
	Gyro Performance	68
APPENDIX A	GG159D GYRO TEST PROCEDURES	

## LIST OF ILLUSTRATIONS

Figure		Page
1	Cutaway View of the Honeywell GG159 Miniature Gas Bearing Gyro	3
2	GG159 Gyro Outline Dimensions	4
3	GG159 Gyro Schematic Diagram	5
4	GG159 Gyro Axes and Phasing	6
5	Gyro Drift Rate History	11
6	Photograph of Materials Undergoing 200-Hour Immersion Test in Fluorolube Flotation Fluid	17
7	Modified Gimbal (below) and Old Style Forked Gimbal (above).	31
8	Old Style Pump Stator Joint (above) and New Style Joint (below).	32
9	Old Style Hysteresis Ring (above), New Style Hysteresis Ring (below)	34
10	Fluid Torque Stability of Experimental (Dummy) Gyro After 300° F Temperature Soaks, OAV	38
11	GG159D1 Anisoelastic Coefficient Comparison	42
12	GG159D1 Attitude Angle Coefficients	42
13	Spinmotor Torques at 185° F and 40 Volts per Phase	47
14	Spinmotor Torques at 120° F and 40 Volts per Phase	48
15	Slot Bridge Deformation	49
16	Cross-Section View of Pump Stator and Windings	54
17	DGG159D1 Anisoelastic Drift Coefficients	57
18	DGG159D Gyro Attitude Angle Drift Coefficient	58
19	Gyro Drift History	

## LIST OF TABLES

Table		Page
1	Drift Rate Shifts and Random Drift	12
2	Corrosion Tests of Metals	16
3	Corrosion Tests of 7636 Flex-Lead Material	16
4	Bond Test Strengths	21
5	Corrosion Tests of O-Rings	24
6	Compression-Set of O-Ring Material	25
7	Dimensional Stability of 6061 Aluminum and 7075 Aluminum (in microinches)	27
8	Drift Rate Stability of the Experimental Gyro After 300° F Temperature Soaks, Output Axis Vertical	37
9	Measured Concentricities of Spinmotor Parts	49
10	Slot Bridge Concentricity	51
11	Slot Bridge Concentricities	52
12	OA Vertical Random Drift (Deg/Hr)	61
13	IA Vertical Random Drift (Deg/Hr/g)	62
14	Synchronous Speed Characteristics	66

## SECTION I INTRODUCTION

This final report is submitted in partial fulfillment of JPL Contract No. 950769. The objective of this study program was to determine the performance degradation of a GG159D-1 gas bearing spinmotor gyro after being thermally sterilized at 300°F for 36 hours. The following was accomplished during the program:

- An extensive analysis and design study was conducted to determine the optimum materials required for the GG159D-1 gyro.
- The GG159 gyro design was further developed and modified to accommodate the materials changes and withstand the 300°F environment.
- An experimental gyro (without spinmotor) was fabricated and tested to evaluate the materials and design changes during sterilization cycling. (The new style H-ring and gimbal configuration could not be evaluated during this Phase.)
- One GG159D-1 gyro was fabricated and tested. Gyro performance was evaluated throughout five thermal sterilization cycles.

The reference for the GG159D-1 design was the GG159C gyro. The GG159C gyro was known to have limited 300°F storage capability due to the breakdown of the flotation fluid and the melt temperature of the balance eutectic alloy at temperatures less than 300°F. Other problem areas were uncovered and defined throughout this study and development program.

## SECTION II

### PHYSICAL DESCRIPTION OF THE GG159 GYRO

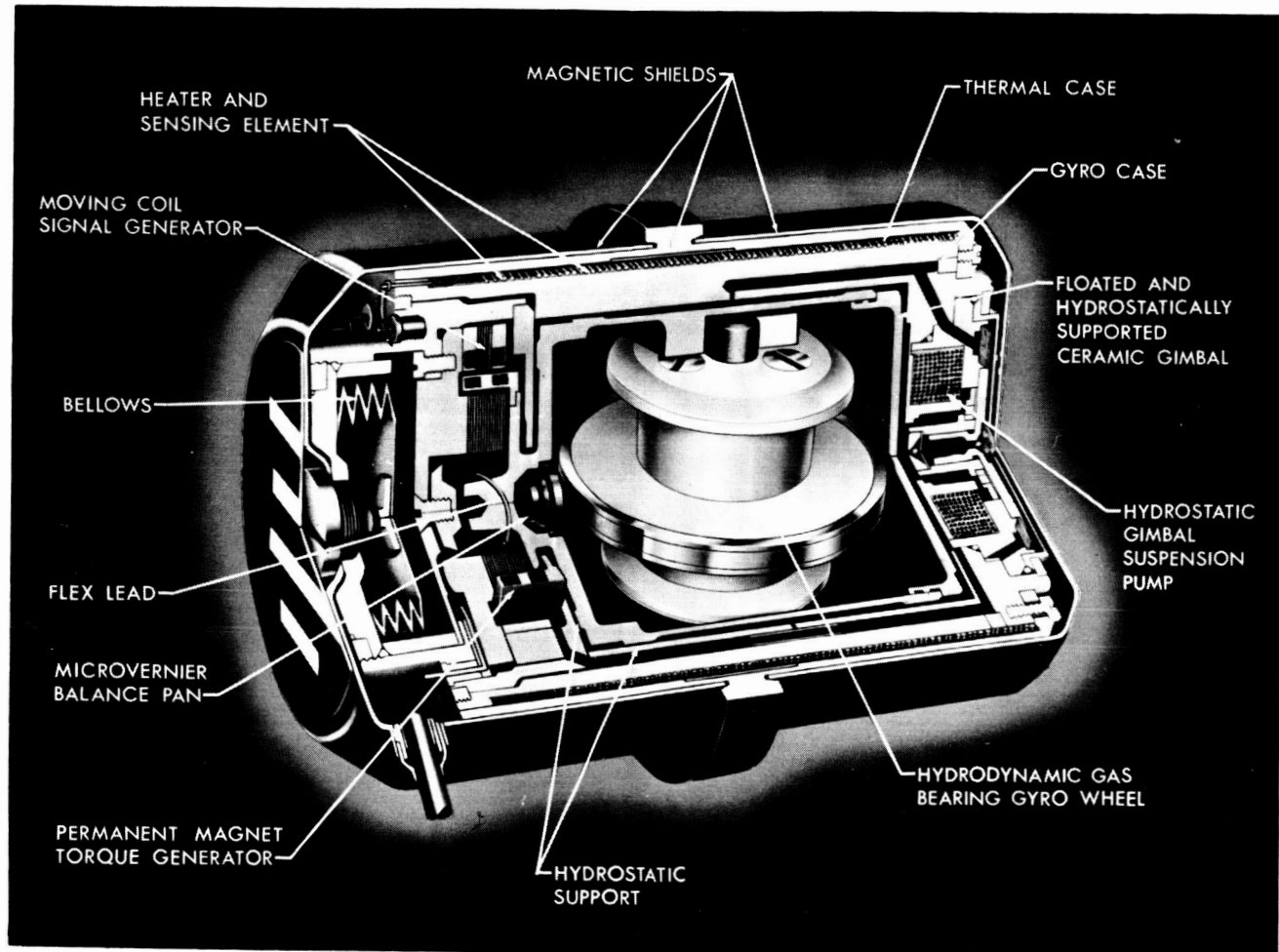
The GG159 is a small single-degree-of-freedom floated gyro for use in rate measurement, attitude reference, and platform stabilization applications.

Principal features of the GG159 include:

- Hydrodynamic gas bearing spinmotor with angular momentum of  $1 \times 10^5$  cgs units.
- Non-contact hydrostatic bearing on the gyro output axis.
- Moving coil permanent magnet torque generator.
- Microvernier balance pan for adjustment of the g-sensitive drift terms.

A cutaway view of the GG159 gyro is shown in Figure 1. Outline dimensions are shown in Figure 2. Figure 3 is a schematic diagram and Figure 4 shows gyro axes and phasing.





G-020

Figure 1. Cutaway View of the Honeywell GG159 Miniature Gas Bearing Gyro

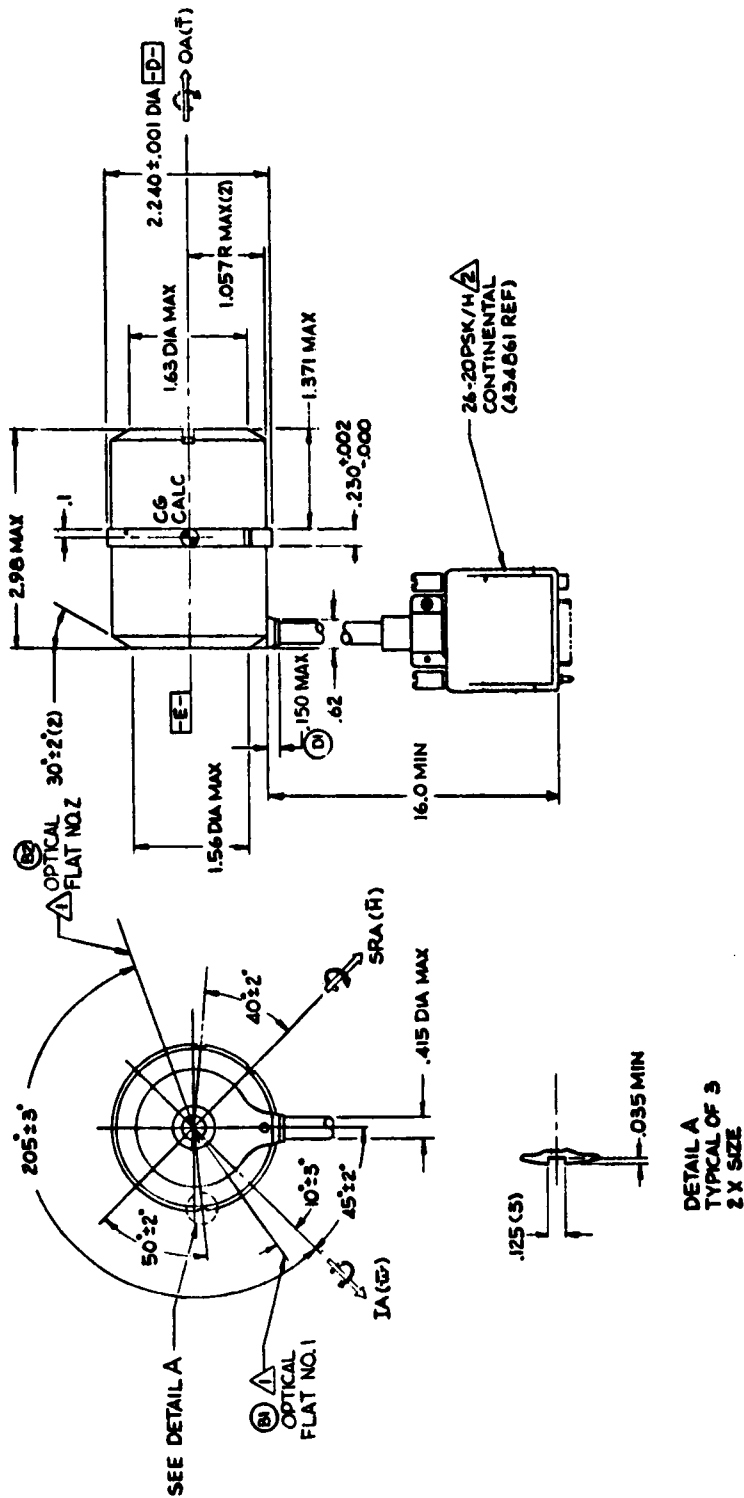


Figure 2. GG159 Gyro Outline Dimensions

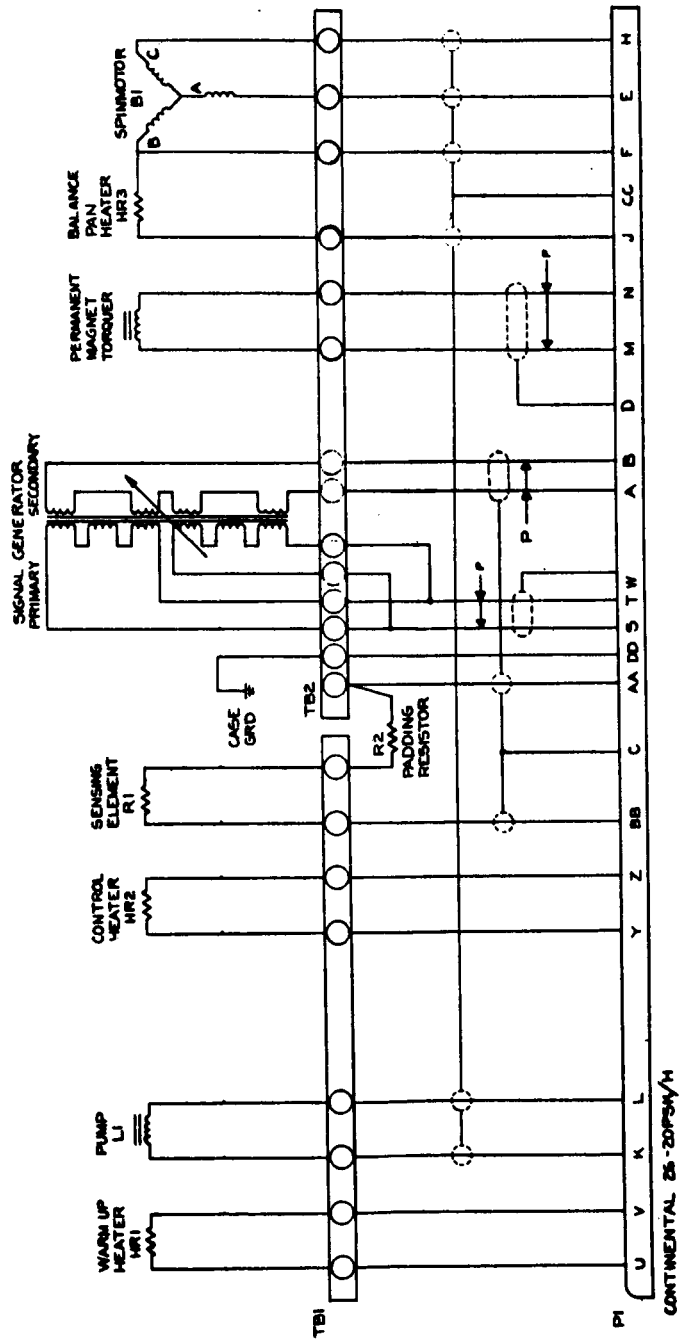


Figure 3. GG159 Gyro Schematic Diagram

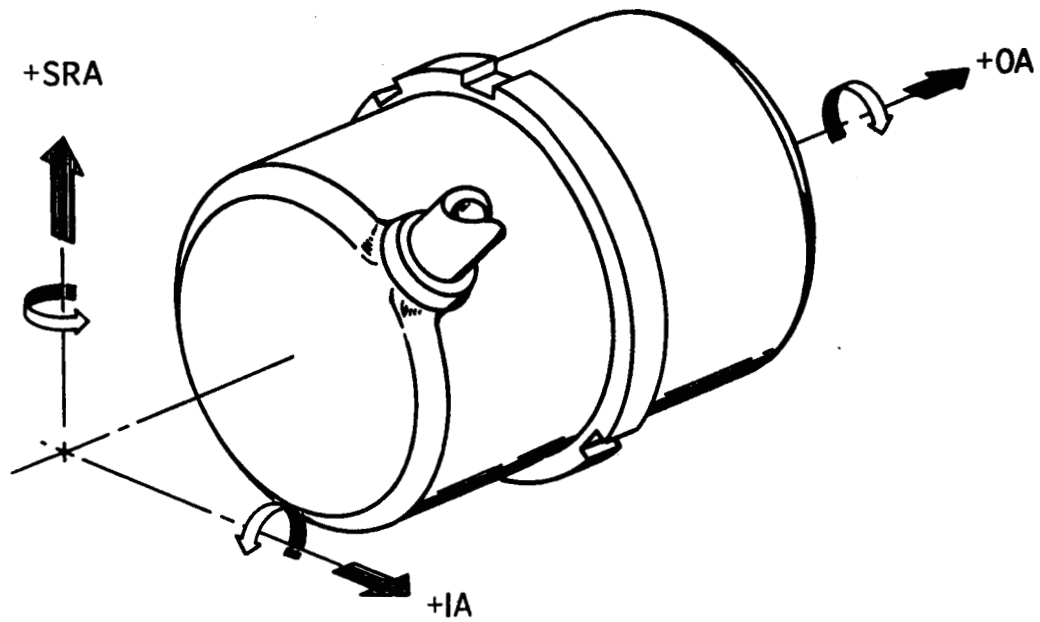


Figure 4. GG159 Gyro Axes and Phasing

### SECTION III SUMMARY

The results of this program are summarized in the following subsections:

- Materials study and gyro development
- Spinmotor failure and corrective action
- Final gyro performance.

#### MATERIALS STUDY AND GYRO DEVELOPMENT

##### Materials Study

The flotation fluid was changed from Bromolube to Fluorolube after stability and corrosion effects were determined for a 300° F environment. 200-hour and 1000-hour tests were completed using visual corrosion effects and weight changes of materials in contact with the lube as judgment criteria. Results were positive and no material changes were deemed necessary.

The flex lead material was changed from alloy 7636 to alloy 6148 (silver-copper) because the higher forming temperature of 450° F added to the torque stability. As corrosion tests of alloy 6148 in Fluorolube at 400° F had been previously completed with positive results these tests were not repeated.

Epoxy adhesives used throughout the gyro for bonding and filter material were changed from the 6020 series to the 6293 series because of their known increased strength at 300° F. Simulated joint configurations were subjected to 10 sterilization cycles and tested for bonding strength. In all cases where the epoxy was used for bonding the tensile strength was over 1000 psi.

The solder used throughout the gyro for completing electrical circuits was changed from spec 6570 (melting point -350° F) to spec 6225 (melting point -450° F).

The GG159 gyro uses one O-ring for separating fluid flow paths. The material for this O-ring was changed to A710B (silicone rubber) after determining that the compression-set of this material, after 10 sterilization cycles, was less than the other materials tested.

The balance ring material was changed from "Heavimet" to tantalum because testing, independent of this study program, indicated tantalum was much more resistant to lube absorption.

The eutectic used in the balance pan was changed to a 63 percent tin and 37 percent lead alloy. The melting range of this alloy was found to be 365° F to 361° F.

The material for the gyro case was changed from 7075 aluminum to 6061 aluminum. Dimensional stability testing of 10 sterilization cycles on sample gyro cases showed approximately an order of magnitude improvement.

The insulation material on the wire used for the signal generator primary and the balance pan was changed after reviewing all the wire types used throughout the gyro against manufacturer's specifications. The criteria was to provide maximum dielectric strength at 300° F.

#### Gyro Development

The gyro gimbal was redesigned to provide flotation in the lower density Fluorolube. The same gimbal size was retained while the weight was reduced by eliminating the "fork" arrangement of the old-style gimbal.

The hydrostatic gimbal pump assembly was modified to provide a mechanical joint after it was discovered the assembly would come apart during 300° F temperature cycling.

The method of mounting the hysteresis ring within the spinmotor rotor was changed to a compliant shrink fit to reduce stresses induced during sterilization cycling.

#### SPINMOTOR FAILURE AND CORRECTIVE ACTION

Following initial build of the GG159D-1 gyro, the spinmotor failed to start after the third sterilization cycle. When the spinmotor was disassembled it was discovered that the stator slot bridge had deformed enough to interfere with the rotor, thus causing failure to start.

After a stress analysis of the stator assembly was completed the stator end shields were changed from stainless steel to Inconel 600 material and the epoxy backfill was eliminated. Dimensional stability measurements over sterilization cycling indicated the deformation problem had been solved. This was confirmed when the gyro was rebuilt with the modified stator assembly and subsequently successfully subjected to five sterilization cycles.

#### FINAL GYRO PERFORMANCE

The final DGG159D-1 gyro assembly was tested throughout five sterilization cycles (300° F for 36 hours) to determine gyro performance. The results are summarized below.

### Drift Stability and Random Drift

The g-sensitive and g-insensitive drift rates and the random drift of the gyro were determined initially and after each sterilization cycle. A summary of the drift rate shifts and the random drifts is tabulated in Table 1.

The magnitude of the gyro drift terms throughout the testing is shown in Figure 5.

### G<sup>2</sup> Drift Coefficients

The measured anisoelastic g<sup>2</sup> coefficient was 0.06 degree/hr/g<sup>2</sup> maximum over the vibration frequency range of 20 to 2000 cps.

The maximum value of the attitude angle g<sup>2</sup> coefficient was 0.03 degree/hr/g<sup>2</sup>.

### Spinmotor Runup-to-Runup Stability

OA vertical runup-to-runup stability was measured initially and after the first and fifth sterilization cycles. The RMS value for 5 cycles each was:

Initial	-	0.011 degree/hr
First cycle	-	0.007 degree/hr
Fifth cycle	-	0.000 degree/hr

### Null Repeatability and Elastic Restraint

Measured Gyro null repeatability	-	0.01 degree/hr max.
Measured elastic restraint	-	0.038 degree/hr/mr



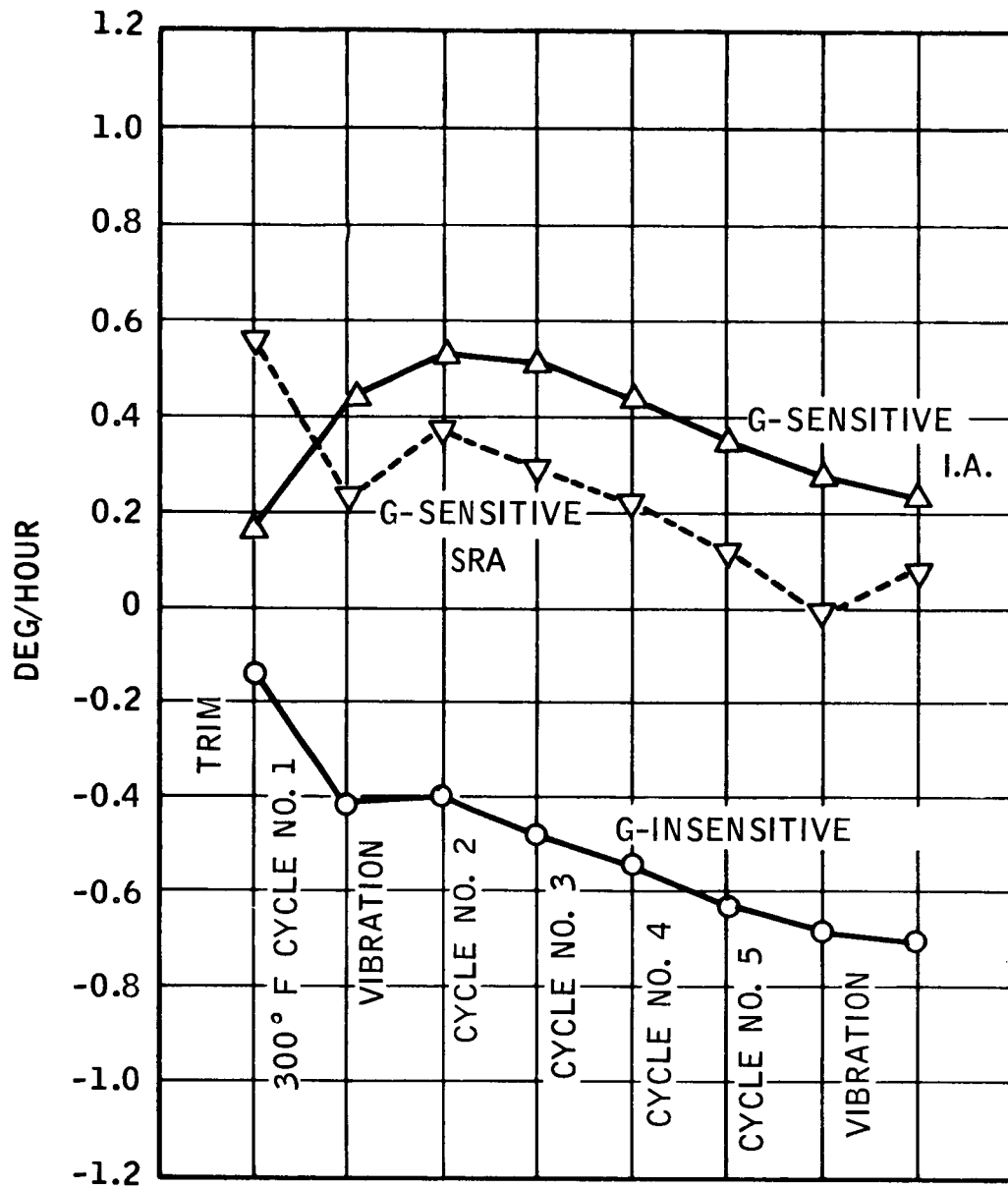


Figure 5. Gyro Drift Rate History

Table 1. Drift Rate Shifts and Random Drift

Cycle Number	Drift Shifts (deg/hr)			Random Drift deg/hr 4 hr, 1 $\sigma$	
	g-insensitive	g-sensitive IA	g-sensitive SRA	OAV	IAV
Reference	---	---	---	0.003	0.002
1	-0.26	0.26	-0.34	0.003	0.002
2	-0.07	-0.02	-0.09	0.001	0.001
3	-0.07	-0.08	-0.07	0.001	0.002
4	-0.09	-0.08	-0.10	0.001	0.002
5	-0.04	-0.08	-0.13	0.002	0.003

## SECTION IV MATERIALS STUDY

Purpose of the materials analysis and design study was to determine the optimum materials to use in the GG159D-1 gas bearing gyro. The results of this study also indicated those materials not suitable for the 300° F thermal sterilization which would have to be changed.

The areas of investigation were:

- Gimbal flotation fluid
- Adhesives (solders and epoxies)
- O-Rings
- Balance rings
- Eutectic alloy, balance pan
- Gyro case material
- Wire insulations

### GIMBAL FLOTATION FLUID

The GG159C gyro uses a Bromolube flotation fluid which has a density greater than 2.0 gms/cc. Before starting this development program it was established that Bromolube fluid would not be satisfactory for use in gyros requiring 300° F sterilization because of the fluid's chemical breakdown temperature (285° F) with resulting corrosion tendencies.

Kel-F 10 Fluorolube was selected for further study because it was known to be less corrosive, provided maximum density (other than Bromolube) and the viscosity required in the GG159D-1 gyro. Kel-F 10 oil is a conventional trifluorochloroethylene damping fluid procured from Minnesota Mining Co.

In order to determine if Kel-F Fluorolube was suitable for use in the GG159D-1 gyro the following areas were investigated.

- The physical specifications such as pour point, viscosity, cloud point, fracture point and volatility.
- Corrosion effects on materials in contact with the fluid.
- The stability of fluid viscosity with 300° F sterilization cycling.

#### Physical Specifications

The following physical characteristics of the Fluorolube fluid were determined using standard laboratory procedures:

##### 1) Viscosity and Density

<u>Temperature</u>	<u>Viscosity, Cp</u>	<u>Density, gms/cc</u>
100	52.2	1.938
160	57.6	1.887
180	34.2	1.808
185	30.2	1.866

$$\text{Density slope} = 8.44 \times 10^{-4} \text{ grams/cc/° F}$$

$$\text{Expansion} = 4.52 \times 10^{-4} \text{ cc/cc/° F}$$

##### 2) Cloud Point +12° F

- 3) Pour Point +5° F
- 4) Fracture Point -86° F
- 5) Volatility

Test conditions - +200° F, 72 hours, open beakers

Results - the viscosity increased 7.3 percent to 61.8 centipoise as measured at +160° F.

Kinematic viscosity was measured per American Society for Testing Materials (ASTM) D-445 using Cannon-Ubbelohde viscometers in a temperature bath controlled to  $\pm 0.05^\circ \text{F}$  (precision). Measurements were made with thermometers accurate to  $\pm 0.1^\circ \text{F}$ . Kinematic viscosity was converted to absolute viscosity by multiplying by density as determined in 50 cc Babcock pycnometers with  $\pm 0.001$  gms/cc accuracy and  $\pm 0.0002$  gms/cc precision.

Pour point and cloud point were measured per ASTM D-97.

Fracture point was measured in clean glass test tubes with a thermocouple in the center of fluid mass and cooled at a rate of  $1^\circ \text{F}$  per minute in a liquid bath. The criteria for fracture is visible cracking of solidified fluid.

### Corrosion Tests

The corrosion effects on the metals used in contact with the gyro flotation fluid were determined with the following procedure.

Material samples of brass, 303 stainless steel, 52100 bearing steel, Hipernik, Armco iron (tin plated), plain Armco iron, chromatic aluminum, and 7636 flex lead material were immersed in Fluorolube flotation fluid at  $300^\circ \text{F}$ . These samples were checked at 200 hours and 1000 hours for weight change and discoloration.

Tables 2 and 3 list the results of these tests. Figure 6 is a photo of some of the materials during the test.

Table 2. Corrosion Tests of Metals

Material Immersed in Fluid	200-Hour Test		1000-Hour Test	
	Corrosion	Weight Change	Corrosion	Weight Change
Fluorolube by itself	No change in color or clarity	-	No change in color or clarity	-
Brass (6521)	Slight tarnish	0.005% gain	Slight tarnish	0.01% gain
303 Stainless (6513)	No sign	0.003% gain	No sign	0.01% gain
52100 Bearing Steel	No sign	0.1% loss	Light film	0.01% loss
Hipernik (6536)	Very slight tarnish	0.002% gain	Slight tarnish	0.002% gain
Armco-Iron (tin plated)	No sign	0.01% gain	No sign	0.01% gain
Armco-Iron (6663)	One side showed rust-like film	0.005% gain	Slight tarnish	0.002% gain
Chromate Aluminum	No sign	0.02% loss	No sign	0.003% loss
Infrared Analysis: Spectrographic Analysis:	No organics after 200 hours and 1000 hours Negative			

Table 3. Corrosion Tests of 7636 Flex-Lead Material

Test	Test Conditions	
	200 Hours	1000 Hours
Weight change	22% gain	1.2% gain
Appearance of fluid	No change in color or clarity	No change in color or clarity
Appearance of flex-leads	No sign of corrosion	No sign of corrosion
Infrared analysis	No organics	No organics
Spectrographic analysis	Negative	Negative

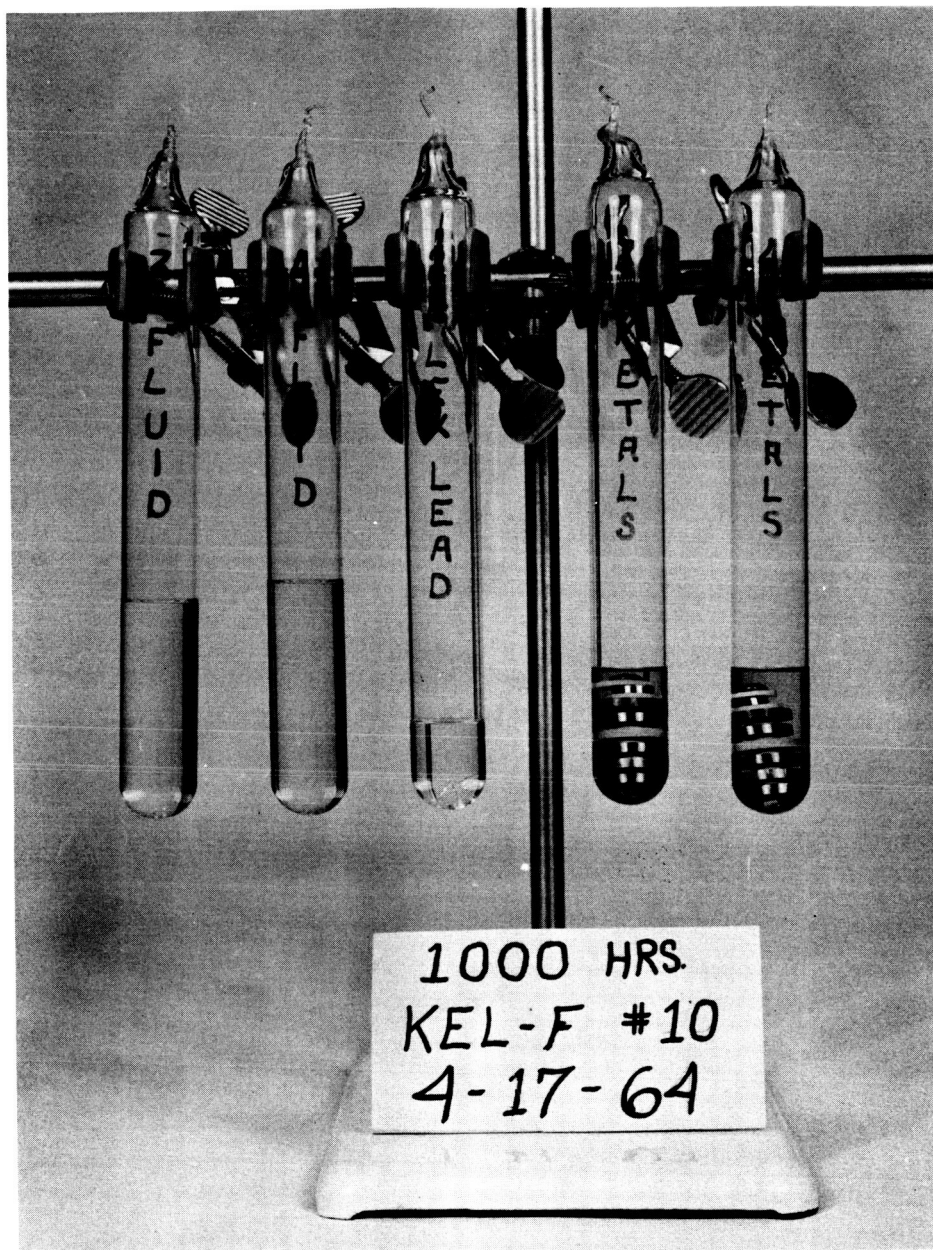


Figure 6 Photograph of Materials Undergoing 200-Hour Immersion Test in Fluorolube Flotation Fluid

Corrosion tests were run in the absence of air by evacuating and sealing glass containers after the specimens were immersed in the fluid. Separate sets of specimens were terminated and examined after 200 hours and 1000 hours at 300° F.

The detailed procedure was:

- a) Cleaned, weighed specimens were placed in glass test tubes and covered with fluid.
- b) Test tubes were necked down by a glass blower.
- c) Tubes were evacuated with a vacuum pump while heated in a water bath to outgas the fluid.
- d) The test tubes were flame sealed while under vacuum.
- e) Test tubes were wrapped in aluminum foil to avoid any possible photo reactions and placed in a 300° F circulating oven.
- f) At the end of the time period all systems were photographed in color.
- g) The tubes were opened with a file, specimens were washed in freon, reweighed, and remeasured.
- h) Clean, dry specimens were rephotographed in color.

#### Fluid Stability

The viscosity of the Fluorolube fluid was measured before and after 200 hours at 300° F. The change in viscosity was 0.6 percent. This change will cause a corresponding percentage change in the gyro damping (C) and therefore the gyro gain (H/C).

Kinematic viscosity was measured per ASTM D-445 in Cannon-Ubbelohde viscometers. The temperature bath was controlled to  $\pm 0.05^\circ \text{F}$  (precision) and measured with thermometers accurate to  $\pm 0.1^\circ \text{F}$ .



## Conclusions

The physical specifications of the Kel-F 10 fluid are satisfactory for use in the GG159D-1 gyro.

In Table 2, brass, Hipernik and plain Armco iron show a slight tarnish. This tarnish is not considered harmful to gyro performance as the fluid remained clear and free of contamination as indicated by the infrared and spectrographic analysis. The weight changes in Table 2 are small and will not affect the stability of the gyro drift terms because the materials are affixed to the gyro case rather than to the gimbal assembly.

In Table 3, the corrosion test results of 7636 (Honeywell Alloy) flex lead material are inconclusive due to the apparent large weight change during the 200-hour test. The factors limiting this material were the forming temperature of 300° F and the test results on the experimental gyro reported in Section VI. The flex lead material selected for the GG159D-1 gyro was 6148 (silver-copper) which is formed at 450° F. 200-hour corrosion tests had previously been completed on the silver-copper alloy in Fluorolube at 400° F during January 1963. The weight gain was 1.9 percent with no visual signs of corrosion. Corrosion tests were not repeated because of these positive documented results of prior testing.

The 0.6 percent viscosity change per 200 hours at 300° F is considered insignificant. This is approximately 0.1 percent change per 36 hour sterilization cycle.

Based on the above conclusions Kel-F 10 Fluorolube was used as the flotation fluid in the GG159D-1 gyro.

## ADHESIVES

Table 4 summarizes the bond test results of those materials held together by epoxy adhesives in the GG159 gyro. These tests were conducted to determine if the tensile strength of the joints was adequate following thermal sterilization cycling at 300° F.

The solder used for making electrical connections within the gyro was changed from spec 6570 with a melting point of 350° F to spec 6225 with a melting point of 450° F. The solder was not tested because the necessary information regarding melting points was readily available in the existing specifications.

### Test Procedures

Test joints and metal butt tensile plugs were fabricated as shown in the sketch below. The ceramic discs were cleaned by the procedure used for ceramic air bearing parts (to water break-free condition). The metal joint surfaces were vapor degreased and sand blasted. Joints were bonded using 50 psi pressure at the recommended cure temperature.

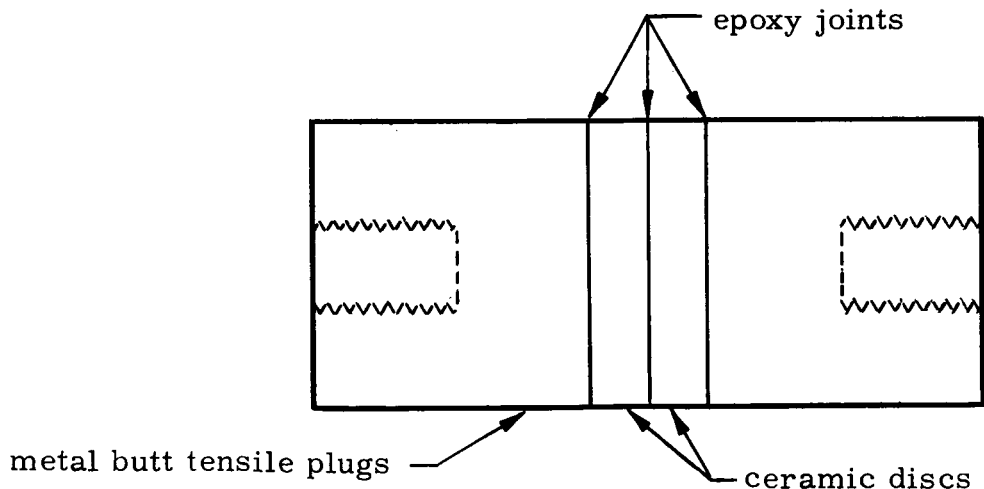


Table 4. Bond Test Strengths

Test Environment: 10 cycles of 300°F for 36 hours  
and room temperature

Materials Bonded	Bonding Agent	Tensile Strength (psi)	Previously Known Strength
Kovar - Lucalox	6293G	2235	1490
Zirconium - Lucalox	6293G	2495	370
Lucalox - 2-micro-finish Lucalox	6293G	2665	
Lucalox - Lucalox	6293G	2360	1510
Simonds No. 81 - Lucalox	7553A	2900	1500
Hypernik - Lucalox	6293G	1285	235
Alnico V - Lucalox	6293N	970	
Zirconium - A203 Ceramic	6293F	5340	
Zirconium - A203 Ceramic	6293J	3690	
Zirconium - A203 Ceramic	6293G	4185	
Tungsten - A203 Ceramic	6293F	5980	
Tungsten - Lucalox	6293G	4210	2460
A203 Ceramic - A203 Ceramic	6293F	3735	

Each sample was subjected to 10 cycles of sterilization temperature (300° F) for 36 hours. Each cycle started and ended at room temperature.

The samples were pulled on the Tinius-Olson testing machine at room temperature using a crosshead speed of 0.050 inch/min. The results tabulated in Table 4 are an average of five sample joints for each combination of materials.

The last column in the table lists values from similar previous tests after five thermal cycles from 200° F to -65° F.

### Conclusions

A bonding strength of 1000 psi is adequate whenever epoxy is used for making a joint. In the case of the Alnico V - Lucalox the 6293N is used as a filler material and a bonding strength of 970 psi is more than sufficient.

The higher values noted after 300° F cycling are possibly caused by diffusion of the materials, with a resulting increase in bonding strength. At any rate, the values following 300° F temperature cycling are more than adequate and the bonding agents tabulated in Table 4 were used in the build of the GG159D-1 gyro.

The high temperature solder spec 6225 will provide adequate electrical connections to withstand the sterilization cycling (300° F).

### O-RINGS

Although no O-rings are used as hermetic seals in the GG159 gyro, one O-ring is used to separate fluid flow within the gyro. Therefore, corrosion and compression set tests were completed on three types of silicone rubber O-rings.

These three types were selected for further investigation after reviewing literature and contacting suppliers. These materials differ in the curing agents used and in the curing temperature.

Table 5 shows the corrosion data of the O-ring materials and Table 6 indicates the results of the compression-set testing.

### Test Procedures

O-ring corrosion tests were completed using the procedure detailed in the Gimbal Flotation Fluid section. Compression set testing was accomplished per ASTM-D-395B with constant deflection.

### Conclusions

Close study of the test results and reflection on the required service of this O-ring leads to the conclusion that, for several reasons, the lowest compression set should govern the choice. Much of the O-ring is in contact with metal rather than fluid which will probably reduce the rate of embrittlement. Also, it is important that the O-ring maintain contact with the mating surfaces to provide the seal. For this reason the low compression set is desirable. It should be noted that the length of time in which the material was exposed to 300° F was extreme. For anticipated gyro sterilization the total required exposure time is considerably less than 1000 hours which means that type A710B (S2-096) material should be used.

Table 5. Corrosion Tests of O-Rings

Material	Test Conditions	
	200 Hours	1000 Hours
<b>Red O-Ring Stock A710-A(S2-096)</b>  Weight change Thickness change Hardness change Fluid appearance  Infrared analysis Spectrographic analysis	32% gain 9% greater 16% loss No change in color or clarity  Large trace silicone Large trace silicone	30% gain 1.9% loss No reading - crumbled Clear - amber in color   
<b>Red O-Ring Stock A710B(S2-096)</b>  Weight change Thickness change Hardness change  Fluid appearance  Infrared analysis Spectrographic analysis	30% gain 10% gain 18% loss  No change in color or clarity  Large trace silicone Large trace silicone	36% gain 3% loss No. 1: 13% greater No. 2: Crumbled Clear - amber in color   
<b>White O-Ring Stock 610A(LS-63)</b>  Weight change Thickness change Hardness change Fluid appearance  Infrared Spectrographic	8% gain 1.3% gain 2% loss No change in color or clarity  No organics Small trace silicone	7.8% gain 2.7% gain 28% loss Clear - very light amber color  - -

Table 6. Compression-Set of O-Ring Material

Test Environment: Specimen immersed in fluid,  
under load and subjected to 10  
cycles of 300° F for 36 hours each

Material	Percent of Compression-Set After	
	7 Cycles	10 Cycles
A710A	11	18
A710B	4	7.7
LS63	41	49

#### BALANCE RING

The GG159C gyro has, in the past, used "Heavimet" material for the gimbal balance rings. Development testing independent of this program has indicated that this material absorbs some fluid and may cause a change in gimbal balance. Substitution of tantalum for Heavimet decreased the weight change by a factor of 100. This general product improvement change was implemented into the GG159D-1 gyro.

#### EUTECTIC ALLOY, BALANCE PAN

The melting point of the alloy normally used in the GG159C is below the sterilization temperature of the gyro. A new alloy was required, and the following were used as goals.

- Ideal melting point - 325° F
- Freezing range - 10° F

A solder with a composition of 63 percent tin and 37 percent lead was tested for melting range and wetting capability on the conventional balance pan. Melting range was from 356° F to 361° F, well under the 10° F maximum range set as a goal. The melting temperature was somewhat higher than the ideal 325° F; however, there were no difficulties in supplying the extra heat energy for melting. This factor actually increases the safety margin of the eutectic during sterilization cycling. Wetting of the alloy to the balance pan plating appeared adequate. Several pans were cycled for possible blistering of the plating and magnetic properties changes. Both tests were negative.

## GYRO CASE MATERIAL

During 300° F sterilization cycling dimensional changes of the gyro case would adversely affect gyro fluid torque stability. To determine the optimum case material, sample gyro cases of 7075-T6 aluminum alloy and 6061 aluminum alloy were fabricated. The 7075-T6 alloy is used in the GG159C gyro and is known to age harden at 250° F. The sample cases were subjected to 300° F sterilization cycling and measured at significant places before and after cycling. The results are shown in Table 7.

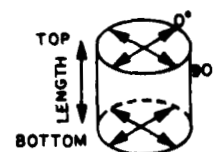
### Test Procedure

The sample gyro cases were 1.25 inches O.D. and 2 inches long with a 0.060-inch wall thickness. Five samples from each material were stress relieved as follows:

- a) 7075-T6 samples - 375° F, 1 hour
- b) 6061 samples - 400° F, 1 hour.



Table 7. Dimensional Stability of 6061 Aluminum and 7075 Aluminum (in microinches)



Test Environment (10 cycles of 300°F to room temperature)	Sample	Top		Bottom		Length	
		0°	90°	0°	90°	0°	90°
6061 Aluminum							
Stress-relieved	1	-130	-110	-220	+ 50	+ 170	+ 190
	2	+ 20	+ 20	+ 10	+ 10	+ 70	+ 70
	3	-120	+ 70	-190	- 40	+ 75	+ 25
	4	+ 30	+ 40	+180	+ 60	- 30	- 20
	5	+ 10	- 20	0	- 80	+ 20	- 30
Not stress-relieved	6	+160	- 70	+ 10	- 70	+ 20	+ 40
	7	- 70	- 80	- 30	-210	+ 30	+ 20
	8	- 10	-120	- 30	- 30	- 110	- 170
	9	- 50	- 20	- 50	- 40	- 40	+ 40
	10	- 60	- 80	-170	- 50	- 20	- 10
7075 Aluminum							
Stress-relieved	17	-130	-260	-580	-240	- 360	- 250
	18	-300	-320	-260	-260	- 430	- 480
	19	-340	-440	-360	-390	- 420	- 580
	20	-610	-750	-670	-890	-1090	- 910
	21	-540	-330	-390	-220	- 430	- 500
Not stress-relieved	22	-500	-270	-350	-300	- 480	- 480
	23	-600	-690	-720	-750	- 710	-1030
	24	-710	-650	-830	-850	- 820	- 800
	25	-710	-520	-790	-510	- 970	-1050
	26	-530	-690	-550	-760	- 990	- 990

Dimensions were measured using a Swiss Microcater with light pressure and a round tip diamond probe. Measurements were made at the points indicated in Table 7. Measurement locations were maintained as consistently as possible throughout the test. Temperature cycling was accomplished automatically in an air circulating oven.

### Conclusions

Comparison of the two materials in Table 7 shows that 6061 aluminum alloy is more stable when exposed to 300°F thermal cycling than the 7075 aluminum. The 7075 allow shrank, almost without exception, an amount varying from 100 to 1000 microinches, as compared to random changes of between 10 to 100 or 200 microinches for 6061 allow, which indicates a stability improvement of from 5 to 10. The stress relieving did not indicate any significant improvement.

The 6061 allow was used in constructing the case of the final GG159D-1 gyro. The fluid torque drift tests results (page 64) indicate that the small random dimensional changes observed in the 6061 allow caused fluid torque drift changes of 0.05 degrees/hour or less.

## WIRE INSULATIONS

A complete study of the wire specifications with regard to the temperature capability of the insulation material was accomplished using wire suppliers' literature. The primary criteria was the dielectric strength of the insulation at 300°F.

### Conclusions

The wire used for the signal generator primary coils was changed from 6436 to 7077 and the balance pan heater wire was changed from 7672 to 7532 to provide additional insulation strength at 300°F. The insulation materials used for all other gyro windings were judged adequate and not changed.

## SECTION V GYRO DEVELOPMENT

The gyro development effort was necessary to (1) adjust the gimbal assembly density for flotation in the lower density Fluorolube and (2) investigate anticipated assembly problem areas.

The areas of investigation were:

- Gimbal flotation
- Pump assembly
- Hysteresis ring

### GIMBAL FLOTATION

The major design modification of the GG159C was due to the change from Bromolube (density ~ 2.10 gms/cc) to Fluorolube (density ~ 1.80 gms/cc). This change required that the gimbal assembly density be decreased accordingly to regain flotation.

A detailed design layout of the gimbal and adjacent components was completed. Two modifications were tried:

- 1) Increase the gimbal size and reduce correspondingly adjacent parts
- 2) Reduce the gimbal weight as much as possible.

The layout study revealed that the best way to reduce the gimbal weight was to remove the fork which connects the motor shaft to the gimbal cup end. After this was done, weight and balance calculations indicated that, with further minor adjustments, the gimbal would be neutrally buoyant in Fluorolube. Design of the gimbal was completed by using shaft mounting and gimbal sealing methods similar to the previous design. Figure 7 shows the GG159C gimbal and the modified gimbal designed for the GG159D.

Primary advantage of this approach is the weight reduction within the gimbal, removing the need to modify any of the adjacent components. A second advantage is improved  $g^2$  drift of the gyro due to isoelasticity of the motor mounting arrangement. This was verified through measurement of  $g^2$  drift on the GG159D (Section VIII). The old gimbal design added a bias to the  $g^2$  drift term of +0.05 to +0.1 deg/hr/ $g^2$ .

The modified gimbal design was adopted for use on the GG159D, and also on other models of the GG159 because of the performance advantages.

## PUMP ASSEMBLY

A pump assembly problem was discovered when standard pumps were subjected to 300°F temperature soaks. The inner stator was pushed out of the outer stator due to the thermal expansion of the pump winding. The parts were modified so that the outer wall could be rolled over to effect a mechanical joint in addition to the epoxy joint. Assemblies of the new configuration successfully withstood the 300°F temperature cycling. The old configuration and the modified configuration are shown in Figure 8.

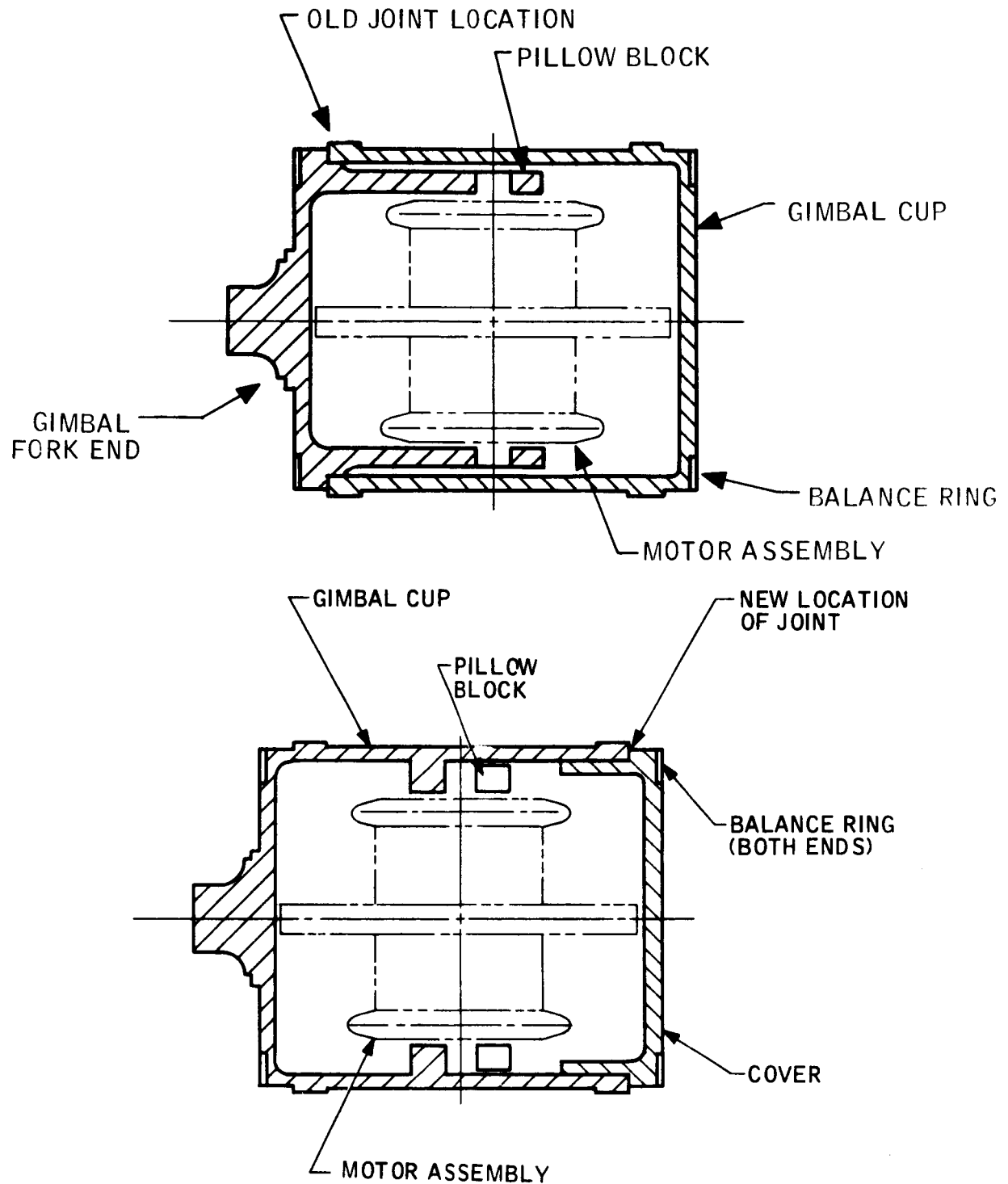


Figure 7. Modified Gimbal (below) and Old Style Forked Gimbal (above).

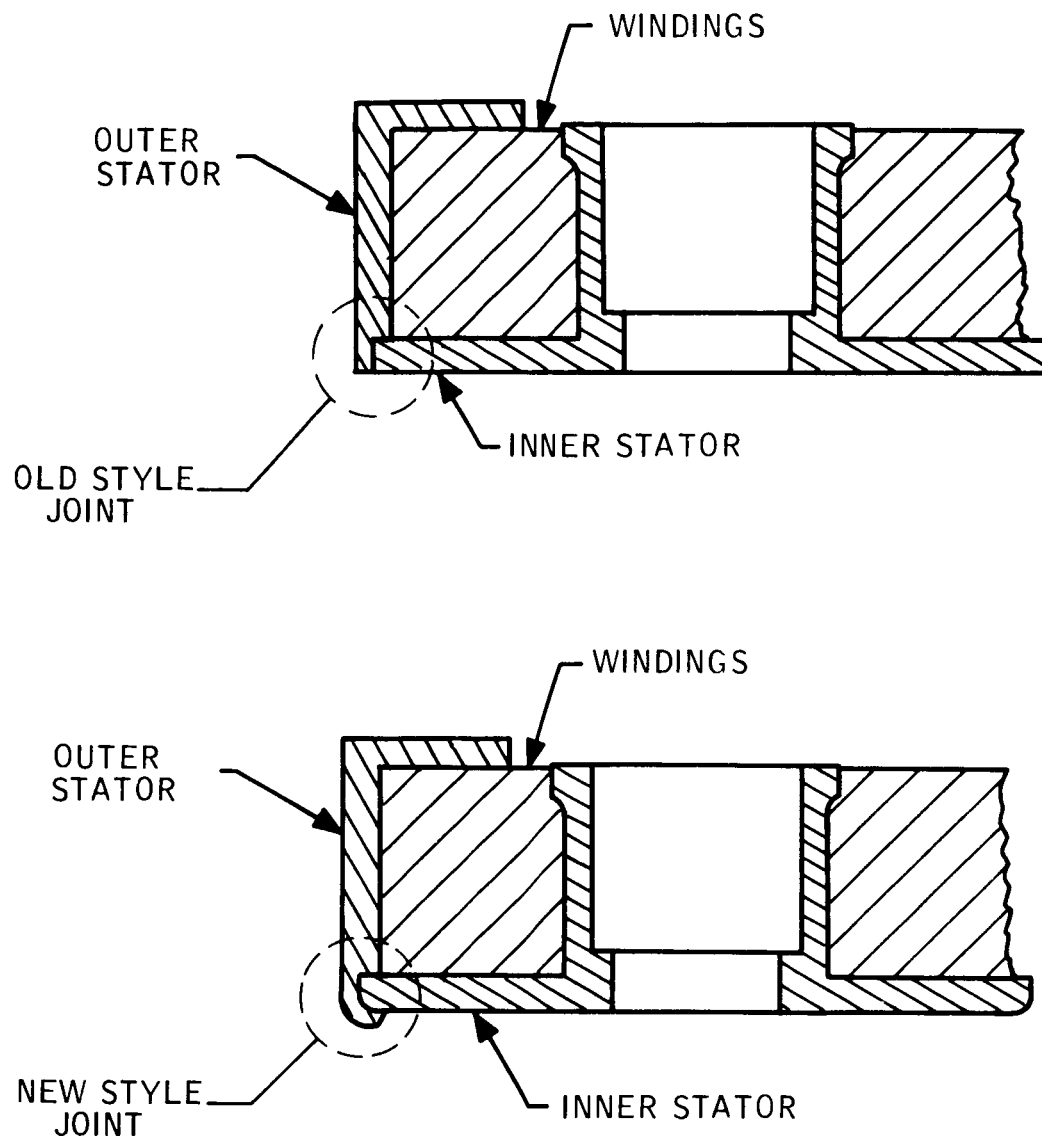


Figure 8. Old Style Pump Stator Joint (above) and New Style Joint (below).

## HYSTERESIS RING

The method of mounting the hysteresis ring within the spinmotor rotor was another area of investigation. The coefficient of thermal expansion mismatch is sufficient to induce high stresses in the "H" ring at 300°F if the ring is mounted in the conventional manner. High stressing of the "H" ring could result in degraded magnetic characteristics and affect spinmotor performance.

The "H" ring was redesigned (see Figure 9) with a thin shrink fit band at each end joined to the "H" ring with a high compliance section. The high stresses are then localized at the 300°F temperature in the end sections. Other advantages of this design are the double support of the ring and the localized contact area to reduce axial slippage.

The ring's magnetic properties were verified by measuring starting and synchronous torque on the first spinmotor assembly using this ring configuration. The spinmotor was subjected to a 36-hour soak at 300°F and the starting and synchronous torques were remeasured. No change of torques was detected.

Radial vent holes were drilled in the "H" ring to allow flushing, cleaning and drying of the narrow cavity between the ring and rotor.

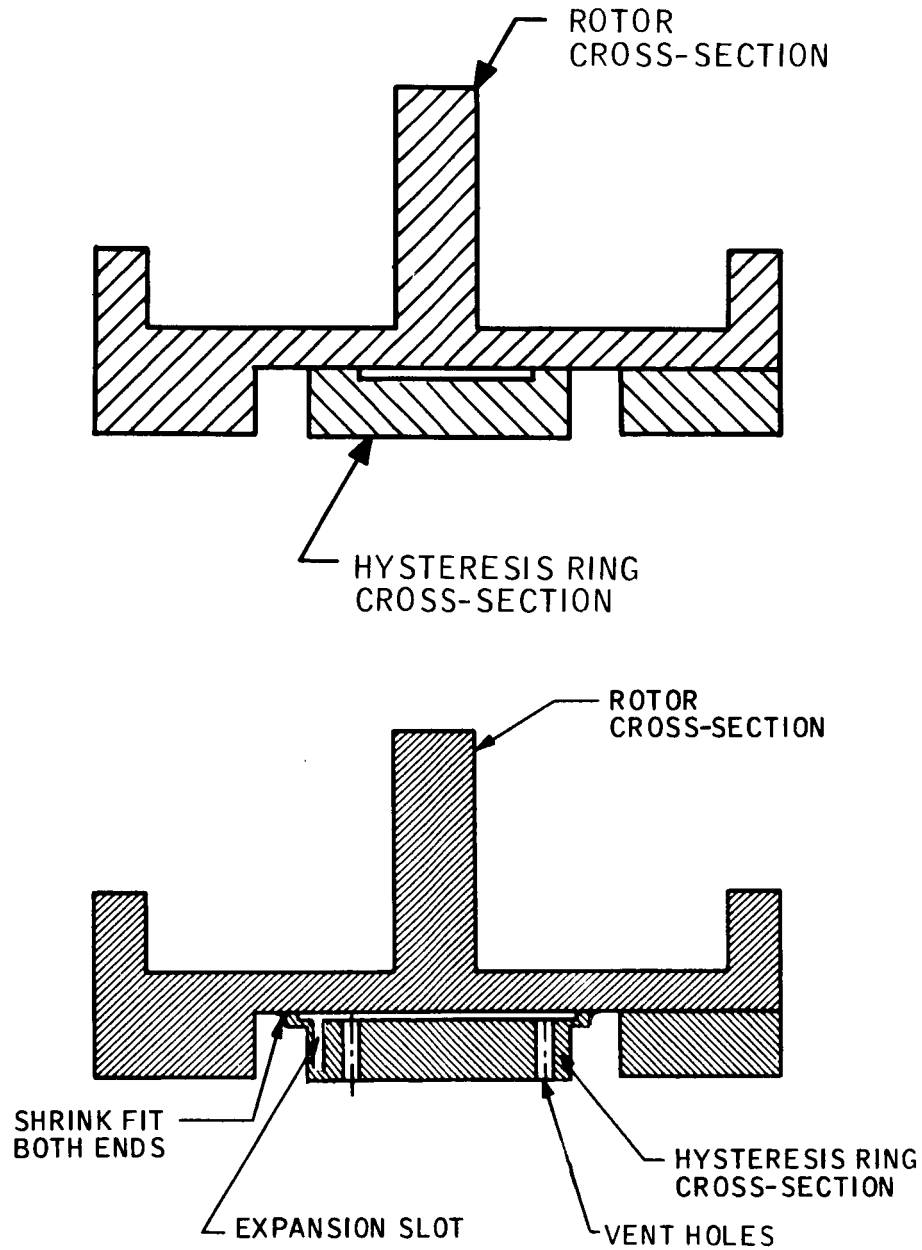


Figure 9. Old Style Hysteresis Ring (above)  
New Style Hysteresis Ring (below)



## SECTION VI EXPERIMENTAL GYRO

The experimental gyro was fabricated and tested for the following reasons:

- To pre-cycle (300° F) the major subassemblies and test them for failures.
- To determine the stability of the g-insensitive drift rate terms.
- To uncover any problem areas during assembly and testing due to noncompatibility of materials, filling techniques, or geometric changes at 300° F temperature.

### GYRO DESCRIPTION

The experimental gyro was fabricated prior to completion of the GG159D gyro spinmotor and gimbal assembly. Therefore, some of the new design changes were combined with standard GG159C parts as follows:

- The case was made from the new 6061 Aluminum Alloy material
- The pump was new style
- The gimbal was GG159C type with a "forked" gimbal
- A zirconium mass was substituted for the spinmotor. The weight was adjusted for neutral bouyancy of the gimbal in Fluorolube.
- The flex leads were 7636 (Honeywell Alloy) in the "spirial" configuration.
- The Header-S.G. assembly was standard
- High temperature epoxies (6293 series) and solders were used throughout.

Subassembly testing and performance testing of this experimental unit produced significant results which were helpful in directing the remaining portion of this development program.

The subassemblies were sterilization cycled to 300° F and tested before and after cycling as follows:

- The header assembly was measured for continuity, leaks, and dielectric breakdown at 500 volts. There was no failure.
- The hydrostatic pump assembly was tested for continuity. There was not failure.
- The case was measured for dimensional stability. The case material was 6061 alloy and shrinkage of this case verified the results of the earlier material study (page 26).
- The gimbal was checked for leak rate, which was less than  $5 \times 10^{-9}$  cc/sec, the maximum allowable for the standard GG159 gimbal assembly. Measurements were made with "Veco" helium detection equipment.

The experimental gyro was assembled, filled, sealed and subjected to five temperature soaks at 300° F. The g-insensitive drift rate terms were measured before and after each temperature soak at 300° F. The results are listed in Table 8 and the fluid torque drift is plotted in Figure 10.

The test procedures used are described in Appendix A. Although torques were actually measured, because the unit had no spinmotor, the data is presented as comparable drift rate for the GG159 gyro have  $H = 1 \times 10^5$  (cgs units).

Table 8. Drift Rate Stability of the Experimental Gyro After  
300°F Temperature Soaks, Output Axis Vertical

Test Number	Time of 300° F Soak (hours)	Total G-Insensitive Drift (deg/hr)		Flex Lead Drift (deg/hr)		Fluid Torque Drift (deg/hr)	
		Magnitude	Shift	Magnitude	Shift	Magnitude	Shift
0	0	-5.54	+1.62	-5.03	+1.49	-0.51	+0.13
1	20	-3.92	+2.45	-3.54	+2.55	-0.38	-0.10
2	39	-1.47	+0.69	-0.99	+0.71	-0.48	-0.02
3	21	-0.78	+0.74	-0.28	+0.75	-0.50	+0.07
4	23	+0.04	-0.38	+0.47	-0.34	-0.43	-0.04
5	21	-0.34		+0.13		-0.47	

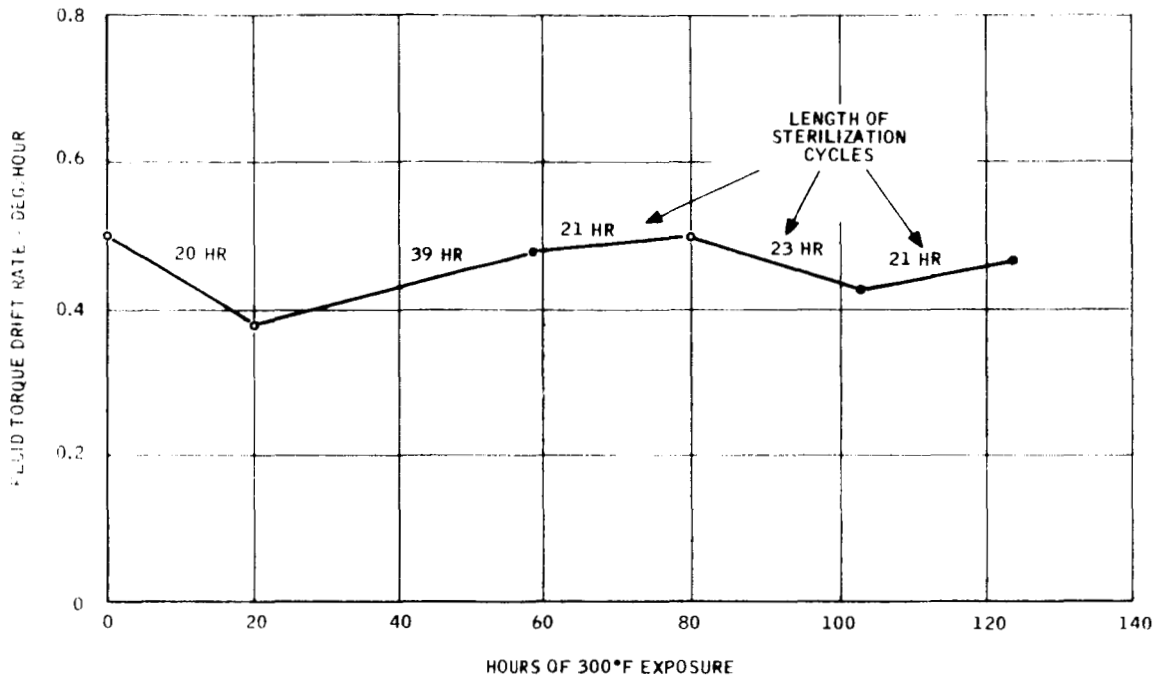


Figure 10. Fluid Torque Stability of Experimental (Dummy) Gyro After 300°F Temperature Soaks, OAV

### Conclusions

The subassemblies maintained functional integrity during 300° F temperature cycling thereby verifying earlier design conclusions.

No problems due to noncompatibility of materials, filling techniques, or geometric changes were discovered, which indicated materials selection and build process were adequate to proceed to the next stage of development.

The stability of the total g-insensitive drift was very poor on this unit and requires further discussion before a conclusion can be reached.

Referring to Table 8, the flex lead drift was initially -5.03 deg/hr and decreased in large shifts with each soak at 300° F. The 7636 flex lead material was formed at 300° F before installation but because of the large initial flex lead drift it must be concluded that the forming was not adequate and the leads were installed in a stressed condition. With each soak at 300° F the leads were stress relieved (annealed). Furthermore, the last shift (-0.34 deg/hr) indicates that this material will never reach a stable condition with 300° F cycling.

As a result of this test data, the flex lead material in the GG159D gyro was changed from 7636 to 6148 (silver-copper alloy). The silver-copper alloy is formed at 450° F, thus minimizing any change in stress (or drift rate) at 300° F.

The fluid torque drift magnitude and shifts shown in Table 8 reflect the relative stability of the gimbal and case material near the fluid gaps. The shifts are both positive and negative, indicating random geometric changes. All but the first shifts are 0.10 deg/hr or less, and the final value after 5 temperature soaks at 300° F is within 0.04 deg/hr of the initial value.

The gimbal and case material stability is sufficient to meet 0.10 deg/hr g-insensitive drift stability per sterilization cycle.

## SECTION VII

### INITIAL GYRO PERFORMANCE

One DGG159D gas bearing gyro was fabricated to determine what the performance degradation would be after being sterilized at 300° F for 36 hours. Materials selection, processes, and design changes derived from previous investigations on this program were implemented on this gyro.

A sterilization cycle, as applied here to the DGG159D gyro, is defined as a 36-hour soak at 300° F followed by a cooldown, over a two hour period to 50° F.

All of the gyro subassemblies were sterilization cycled prior to final assembly. Gyro performance testing was accomplished using the test procedures described in Appendix A.

Gyro performance testing of this unit was terminated following the third sterilization cycle when the spinmotor failed to start. Results of the performance testing, up to the time of the spinmotor failure, are presented in the following paragraphs.

### CALIBRATION AND ADJUSTMENTS

The resistance of the temperature sensor was measured with the gyro in a 185° F water bath. The sensor was then series padded to 780 ohms at 185° F.

The g-insensitive drift was compensated to 0.09 deg/hr.

The g-sensitive drift was adjusted to -0.58 deg/hr SRA and 0.53 deg/hr IA.

## TEST RESULTS

### G<sup>2</sup>-Drift

The gyro was vibrated after calibration and adjustment and again after the first sterilization cycle to measure the anisoelastic drift. The results are shown in Figure 11. Attitude angle drift was measured following initial calibration only (Figure 12).

### Reference Drift Rate

The reference drift rate measured before the first sterilization cycle was:

g-insensitive	-	+0.08 deg/hr
g-sensitive		
IA	-	+0.52 deg/hr
SRA	-	-0.84 deg/hr

### Drift Rate Shift

The gyro drift rate was measured following each sterilization cycle after an eight-hour stabilization period. The sterilization drift rate shift is the difference in drift rate measured before and after the sterilization cycle. Results are tabulated below.

#### Sterilization Drift Rate Shifts

	<u>g-insensitive</u>	<u>g-sensitive</u>	
		<u>IA</u>	<u>SRA</u>
Cycle 1	+0.04° /hr	+0.08° /hr	+0.14° /hr
Cycle 2	+0.01° /hr	-0.07° /hr	-0.15° /hr

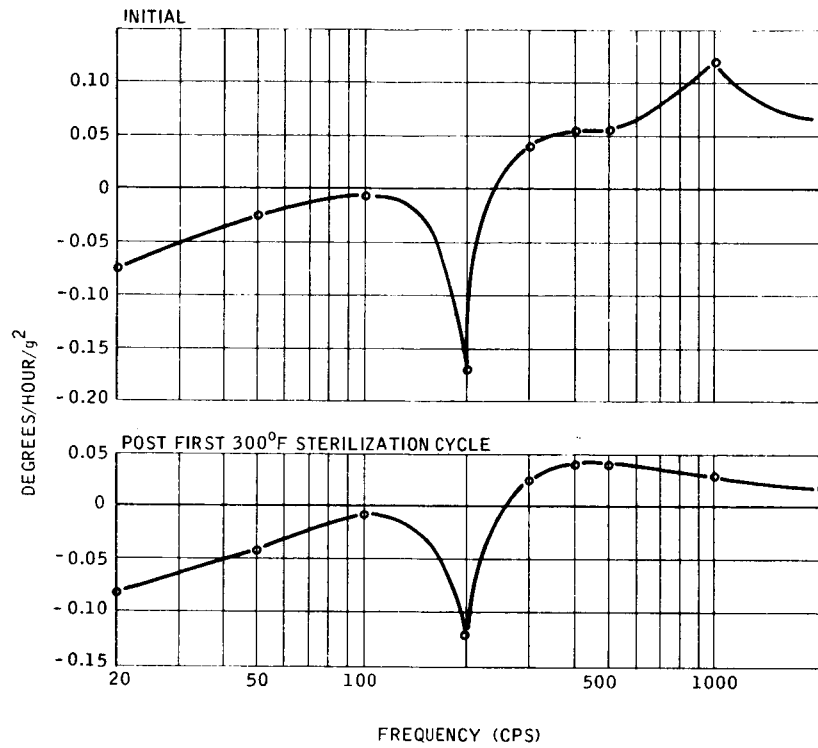


Figure 11. GG159D1 Anisoelastic Coefficient Comparison

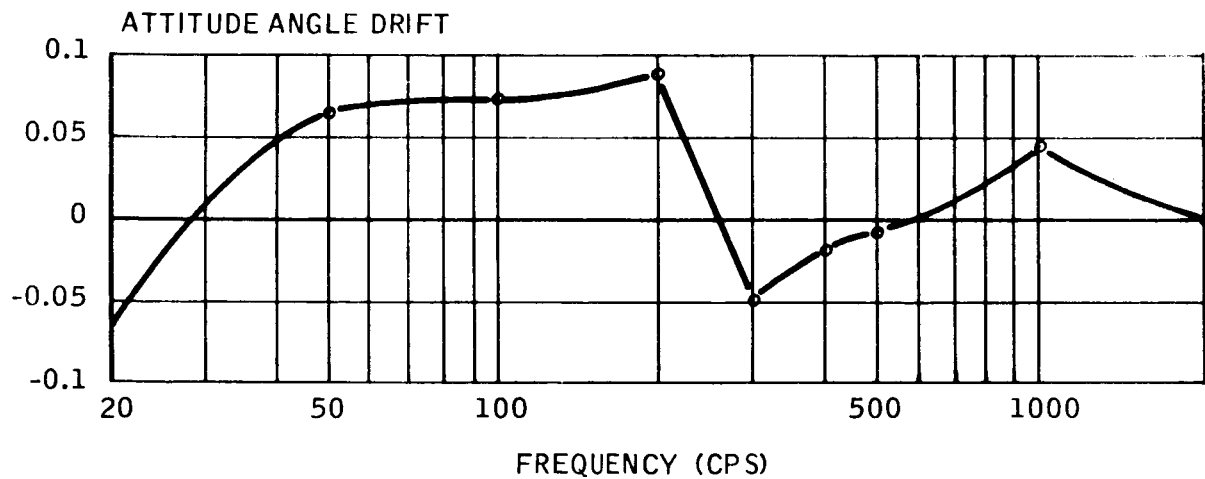


Figure 12. GG159D1 Attitude Angle Coefficients



### Spinmotor Runup-to-Runup Stability

Runup-to-runup stability was measured following the reference drift rate measurement (OAV and IAV) and again after the first sterilization cycle (OAV only). The Drift rate given below is the R.M.S. value of five runups.

	<u>OAV</u>	<u>IAV</u>
Pre-Sterilization	0.009°/hr	0.004°/hr
Post-1st Sterilization	0.008°/hr	

### Random Drift

Random Drift measurements were made after the reference drift and after each sterilization cycle. The test period was four hours for the OAV, IA east and OAH, IA up orientations. Data points were 100 sec integrated drift rate values. One-sigma random drift values were:

	<u>OAV (°/hr)</u>	<u>IAV (°/hr)</u>
Reference	0.005	0.004
Post - 1st Sterilization	0.009	0.004
Post - 2nd Sterilization	0.005	0.008

### Gyro Parameters

Several other gyro parameters measured are listed below:

Signal generator sensitivity	22.8 mv/mr
Torquer scale factor	93.3 deg/hr/ma
Damping coefficient	7720 dcm-sec/rad

Gyro transfer function	296 volts/rad
Elastic restraint	0.006 deg/hr/mr
Null repeatability	0.01 deg/hr max.

### Discussion and Conclusions

The anisoelastic  $g^2$  exceeded the design goal of 0.07 deg/hr/ $g^2$  at several frequencies (See Figure 11) and reached a maximum value of -0.17 deg/hr/ $g^2$  at 200 cps. The reduction of  $g^2$  after the first sterilization cycle was probably caused by the change in effective gas bearing clearances due to the sterilization, which ultimately led to the spinmotor failure.

The  $g^2$  values exceeded the design goal because the running clearances and geometric compensation for half-speed weakness were not completely optimized. Adjustments in these parameters will reduce the  $g^2$  values to below 0.07 deg/hr/ $g^2$ . This was accomplished on the final unit.

The sterilization g-insensitive drift shifts were well within the performance goals of 0.10 deg/hr. The shifts of the g-sensitive values were marginal, and in the case of the 0.15 deg/hr value, slightly exceeded the performance goal of 0.14 deg/hr. The larger shifts were along the SRA and probably were increased due to the dimensional changes within the spinmotor, causing the motor failure following the third sterilization cycle.

Spinmotor runup-to-runup performance was well within the goal of 0.02 deg/hr and indicates results comparable to non-sterilization GG159 gyros.

Random drift was generally within the 0.008 deg/hr performance goal, except for the one isolated case (0.0091 deg/hr). This may have been due to a power supply variation or an external disturbance; however, speculation of this type is not particularly helpful and difficult to precisely establish in the case of isolated happenings.

## SECTION VIII

### SPINMOTOR FAILURE ANALYSIS AND CORRECTIVE ACTION

After the third sterilization cycle the spinmotor of the GG159D gyro failed to start when normal excitation was applied. The motor was started by applying transient high rates about the spin axis by hand while applying excitations. A preliminary failure analysis was made on the completed gyro, and visual inspection and dimensional measurements were accomplished on the motor parts after disassembly. Based on these investigations it was determined that the spinmotor failure was caused by distortion of the stator slot bridge.

After determining the cause of the failure, design analysis and corrective action in the form of design changes were implemented. These changes were verified through build and test of another spinmotor, and subsequent rebuild and test of the gyro.

#### PRELIMINARY FAILURE ANALYSIS

During normal sterilization cycling the spinmotor is started at room temperature and continues running while the gyro is being heated and stabilized to operating temperature. In this case the spinmotor was at room temperature when it first failed to start. Initial testing revealed that if the gyro temperature was incrementally increased to a range of 140°F to 150°F the motor would start with normal excitations applied. This allowed further measurement of the motor operating characteristics.

The spinmotor acceleration torque and load torque was determined by measuring acceleration and deceleration during runup and rundown. Total developed torque was calculated as the sum of the two. Acceleration, load, and total developed torque of the spinmotor at 120° F and 185° F are shown in Figures 13 and 14.

The load torque of 11,000 dyne-cm at synchronous speed is typical for this motor which indicates the gimbal fill gas was of the correct viscosity.

The total developed torque (~11,500 dyne-cm) at synchronous speed has decreased following sterilization cycling. Initial developed torque was ~15,000 dyne-cm. Also, the developed torque decreased as operating temperature was decreased, indicating degraded magnetic performance which has some temperature relationship.

The total rundown time changes from 17 seconds at 185° F to 13 seconds at 120° F. This change was not reflected in increased load torques at synchronous speed. Therefore, the low speed load torques increased with the reduction in temperature.

## FAILURE ANALYSIS

The gyro and spinmotor were disassembled and visually inspected. This inspection disclosed rubbing marks or wear areas on the stator slot bridge. This pinpointed a problem because the manufactured clearance between the slot bridge and hysteresis ring is  $0.001 \pm 0.0001$  inch. Measurements were made with the Indi-ron equipment to determine which element had changed position or shape.

Measured concentricities of the spinmotor parts are shown in Table 9.

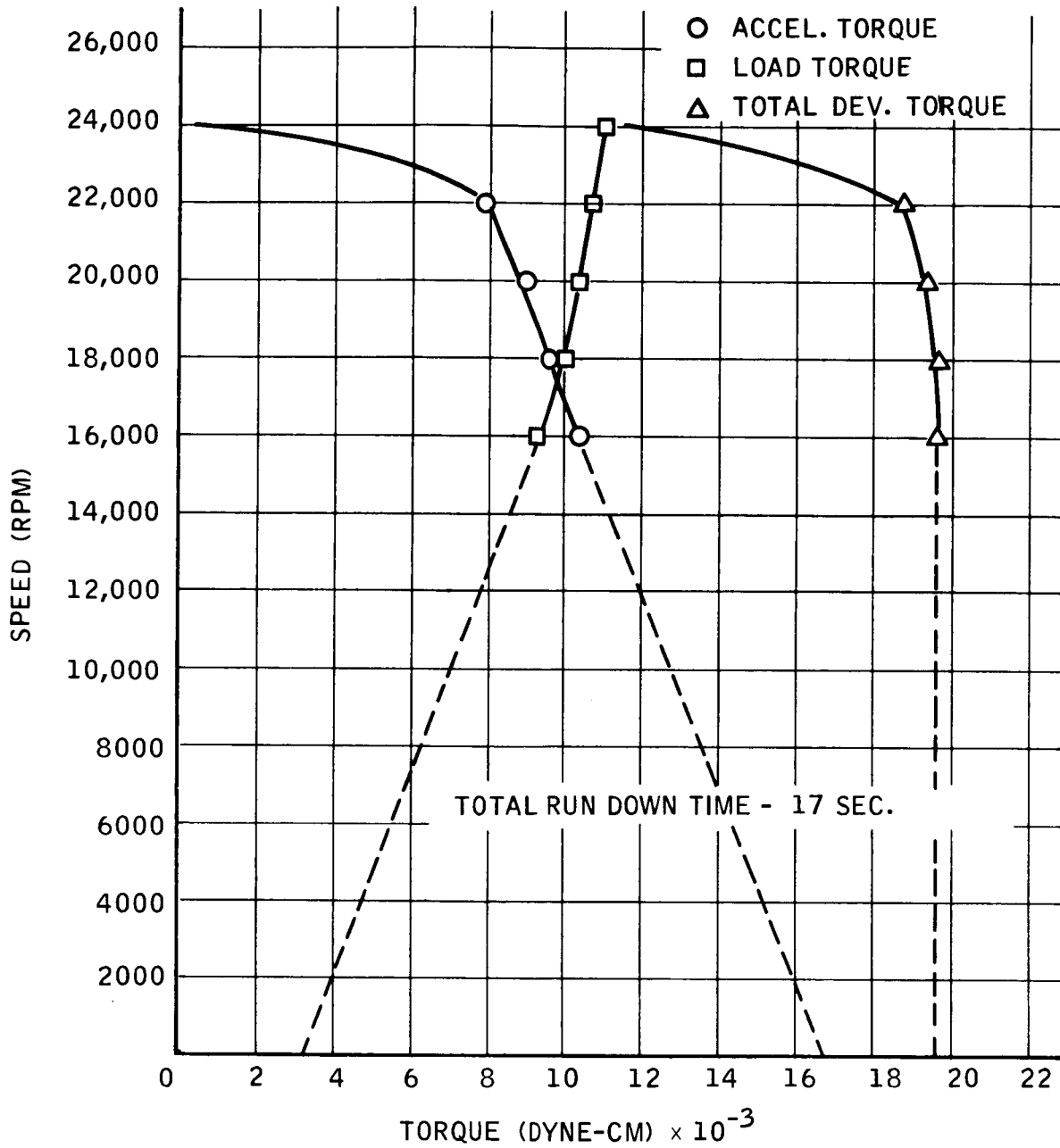


Figure 13. Spinmotor Torques at 185°F and 40 Volts per Phase

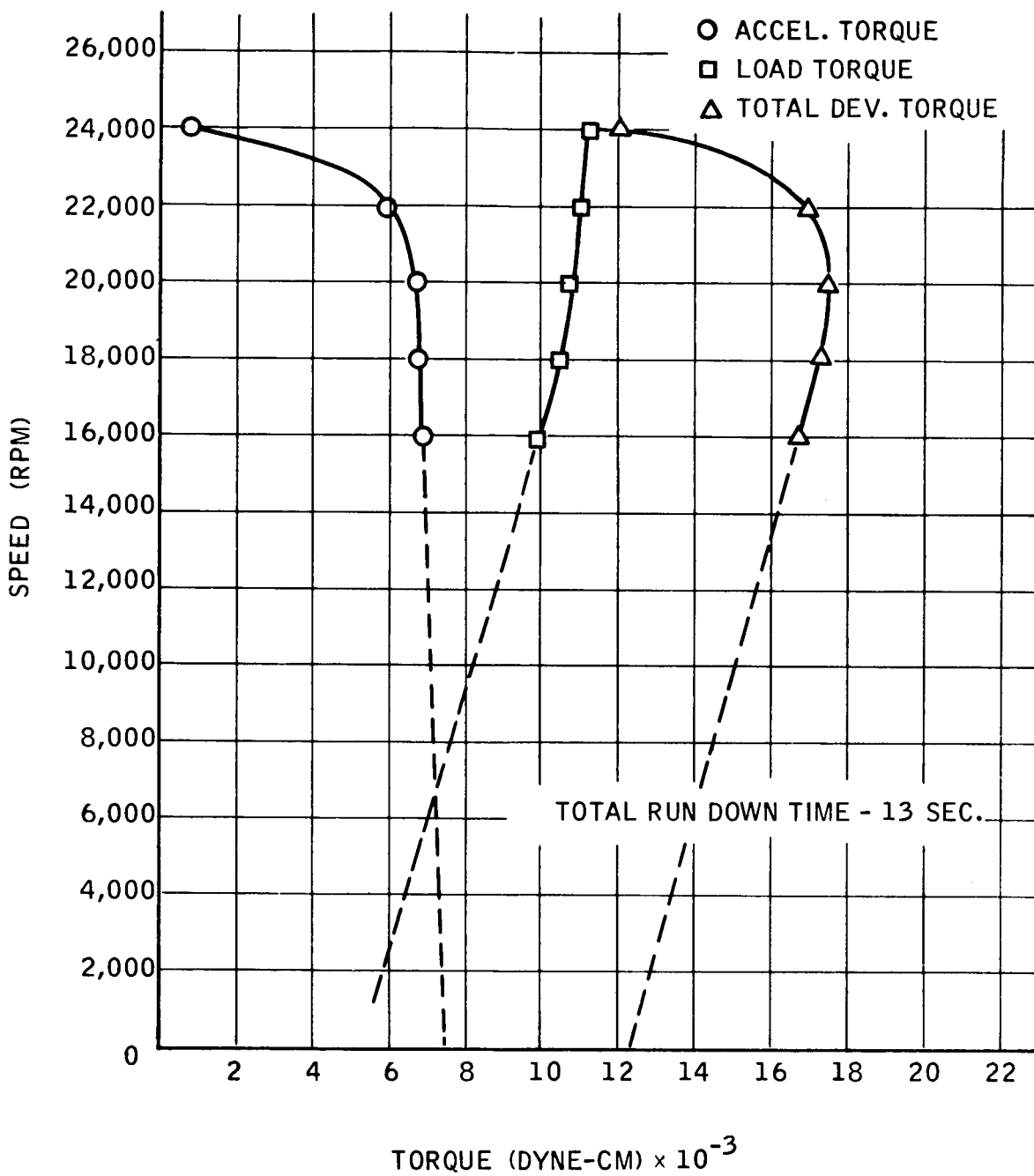


Figure 14. Spinmotor Torques at 120°F and 40 Volts per Phase

Measurement of the diameter of the slot bridge at the wear areas and at the center of the slot bridge showed that the diameter at the wear areas was from 0.0008 to 0.001 greater than at the center (see Figure 15).

Table 9. Measured Concentricities of Spinmotor Parts

Item	Measured Concentricity	Print Tolerances
Rotor Journal Bearings	0.000008	0.000010
Hysteresis Ring	0.000030	0.000100
Shaft Journal Bearings	0.000010	0.000010
Slot Bridge	0.000400	0.000100

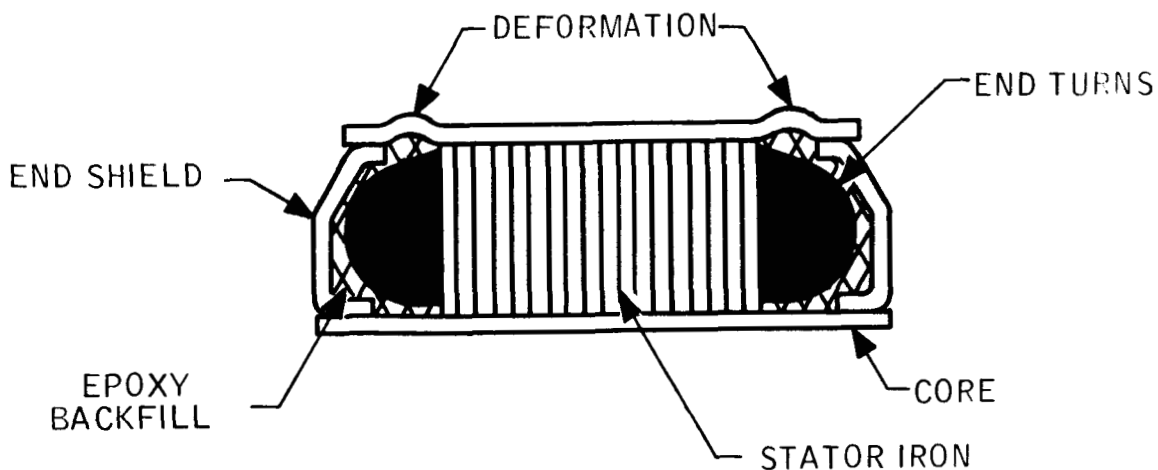


Figure 15. Slot Bridge Deformation

A stress analysis was run on the stator assembly to pinpoint the cause of the deformation. The analysis showed that the axial and radial stresses in the slot bridge material exceed the yield stress. Stresses in the slot bridge for a 230° F temperature excursion are:

Axial stress	65,000 psi
Radial	38,000 psi
Yield stress	22,000 psi

These high stresses are caused by two factors: (1) The epoxy fill between the end shield, and (2) the thermal coefficient mismatch between the hypernik slot bridge and the stainless steel end shield.

The backup shaft and stator assembly from the original build had been processed through the assembly stage, but was not ground.

This assembly was processed to determine the extent of slot bridge deformation on a second assembly. The processing was as follows:

The slot bridge was ground to within 0.0008 inch of the correct size. The assembly was then cycled to 300° F for one hour and an additional 0.004 inch of material was removed. (This interim temperature cycling and a final skin cut on the slot bridge is normal processing for this type assembly.) The shaft assembly was then cycled as follows: 300° F, 36 hours minimum to 40° F, 1 hours minimum. This cycle was repeated for a total of three cycles. The slot bridge concentricity was measured at interim stages with results as tabulated in Table 10.



Table 10. Slot Bridge Concentricity

Processing Stage	Top	Middle	Bottom
After Initial Grinding	0.000030	0.000020	0.000015
One hour, 300°F soak	0.000085	0.000100	0.000260
Second Grind	0.000040	0.000035	0.000045
First Sterilization Cycle	0.000100	0.000090	0.000100
Third Sterilization Cycle	0.000100	0.000220	0.000240

The results of this testing show that the slot bridge does not assume a stable position after the first cycle. A slight deformation can occur on additive cycles as shown in Table 10. This mode of deformation explains why the failure on the original unit did not appear until several sterilization cycles had been completed.

#### CORRECTIVE ACTION

To eliminate slot bridge deformation, the stress levels in the slot bridge must be well under the yield stress. Alternate materials with a lower coefficient of thermal expansion (CTE) must be used. The 400 series stainless steels would be a good choice, except for their magnetic properties. If a magnetic stainless steel is used, some of the air gap flux will be shunted through the slot bridge material. Typically, this will be about a 10 percent reduction in the developed torque per watt of input power. While this is not desirable, it would not eliminate use of magnetic stainless steel.

A more feasible choice was Inconel 600. This material has a CTE of 6.5 in/in/°F. The magnetic permeability is 1.005 in cgs units. A sample lot of this material was purchased and end shields were being fabricated to evaluate a stator assembly. The axial stresses in the slot bridge will be reduced to less than 10,000 psi and the radial stress to under 6000 psi.

Two stator assemblies were fabricated for evaluation with the following changes from the original configuration:

- Inconel 600 end shields
- No epoxy backfill between potted stator windings and end shields.

These assemblies were processed in accordance with normal stator assembly sequence, i. e. :

- Grind OD to within 0.0004 inch of correct size
- Temperature cycle to 300°F
- Grind to final size

Roundness was measured at all stages of processing. These results, along with the readings after sterilization cycling, are shown in Table 11.

Table 11. Slot Bridge Concentricities

Processing Stage	Unit No. 1			Unit No. 2		
	Top	Middle	Bcttom	Top	Middle	Bottom
Initial Grind	20	25	50	30	20	25
1 <sup>st</sup> Temperature Cycle	200	300	400	110	50	120
Final Grind	25	30	30	25	30	30
1 <sup>st</sup> Sterilization Cycle	150	175	175	160	160	350
3 <sup>rd</sup> Sterilization Cycle	150	175	175	160	170	350
6 <sup>th</sup> Sterilization Cycle	180	175	190	180	150	350

NOTE: All readings in microinches

These results show that the slot bridge will assume a stable position after the first sterilization cycle.

In addition to measuring roundness, size was measured to determine if slot bridges were deforming as they did on the unit that failed. The diameter on unit No. 1 was uniform within 40 microinches and within 60 microinches on unit No. 2. The corresponding readings on the original assembly were 800 to 1000 microinches. This indicates that the basic problem is solved.

Based on testing and analysis, the following procedure was used on the rebuild of the sterilization gyro:

- (1) Use of new configuration Inconel 600 end shields
- (2) Eliminate the epoxy backfill, retain an epoxy insulation on the inside of the end shield
- (3) Modify the processing sequence as follows:
  - Grind slot bridge to within 0.0008 inch of correct size
  - Temperature cycle to 300°F
  - Grind slot bridge to within 0.0004 inch of correct size\*
  - Run one sterilization cycle\*
  - Grind slot bridge to the correct size
  - Run three sterilization cycles on the assembly
  - Re-inspect the assembly\*
  - Assemble and check out motor
  - Run three sterilization cycles on completed spinmotor and gimbal assembly
  - Continue into normal gyro build

---

\*Denotes changes from previous processing sequence.

## GYRO RE-BUILD AND PUMP FAILURE

The DGG159D gyro was rebuilt using the same parts, except for the spinmotor and gimbal assembly. After the first rebuild of the unit the drift performance was erratic and the gyro was again disassembled to the gimbal level. A tear-down analysis (standard procedure) indicated that the erratic drift was caused by dielectric breakdown of the pump winding to the pump stator.

The pump assembly was disassembled and the short was traced to a point on the pump inner stator. The breakdown point was a corner radius of the stator as indicated in Figure 16.

A new pump assembly was fabricated.

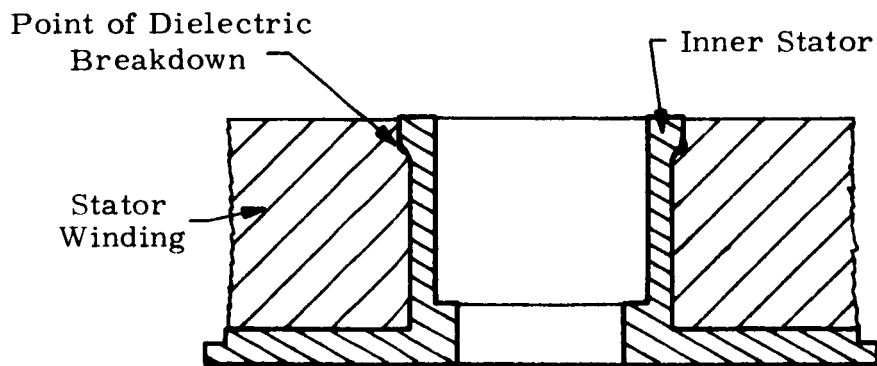


Figure 16. Cross-Section View of Pump Stator and Windings

## DISCUSSION AND CONCLUSIONS

The failure analysis on the spinmotor showed that failure was caused by distortion of the stator slot bridge which "grew" in magnitude with each sterilization cycle until the motor effectively bound up. The distortion of the slot bridge was caused by (1) the epoxy fill between the end shield and end windings, and (2) the slot bridge material having thermal expansion coefficients not matched closely enough to the end shield materials.

Substitution of Inconel 600 end shields and removal of the epoxy backfill has reduced the stress level and the stator distortion with sterilization cycling to a satisfactory level (Table 11).

The dielectric breakdown of the pump winding was caused by a weak point on the inner stator insulation. The inner stator is insulated with three coats of strontium chromate before winding which normally provides adequate dielectric strength. It is possible that the coating was accidentally chipped during the winding process.

Production build of approximately 80 pump assemblies with no dielectric failures indicate that the pump stator is a high reliability unit, therefore it was concluded that this was an isolated failure.

## SECTION IX

### FINAL GYRO PERFORMANCE

The DGG159D gyro was rebuilt with the modified stator and new pump assembly. The testing was conducted to determine what the performance degradation would be after being sterilized at 300° F for 36 hours.

A sterilization cycle as applied here to the DGG159D gyro is defined as a 36-hour soak at 300° F followed by a cooldown over a two-hour period to 50° F. All of the gyro subassemblies, except those used in the previous build, were sterilization cycled prior to final assembly.

Gyro performance testing was accomplished using the test procedures described in Appendix A. Performance testing through five sterilization cycles was completed and the gyro was delivered to JPL.

### CALIBRATION AND ADJUSTMENTS

The resistance of the temperature sensor was measured with the gyro in a 185° F water bath. The sensor was then series padded to 780 ohms at 185° F.

The g-insensitive drift was compensated to -0.13 deg/hr. The g-sensitive drift was compensated to +0.16 deg/hr/g IA and +0.57 deg/hr/g SRA.

### TEST RESULTS

#### G<sup>2</sup> Drift

The gyro was vibrated after calibration and adjustments, and after the first and fifth sterilization cycles to measure the anisoelastic g<sup>2</sup> drift. The results are shown in Figure 17. Attitude angle g<sup>2</sup> drift was measured following initial calibration only (see Figure 18).

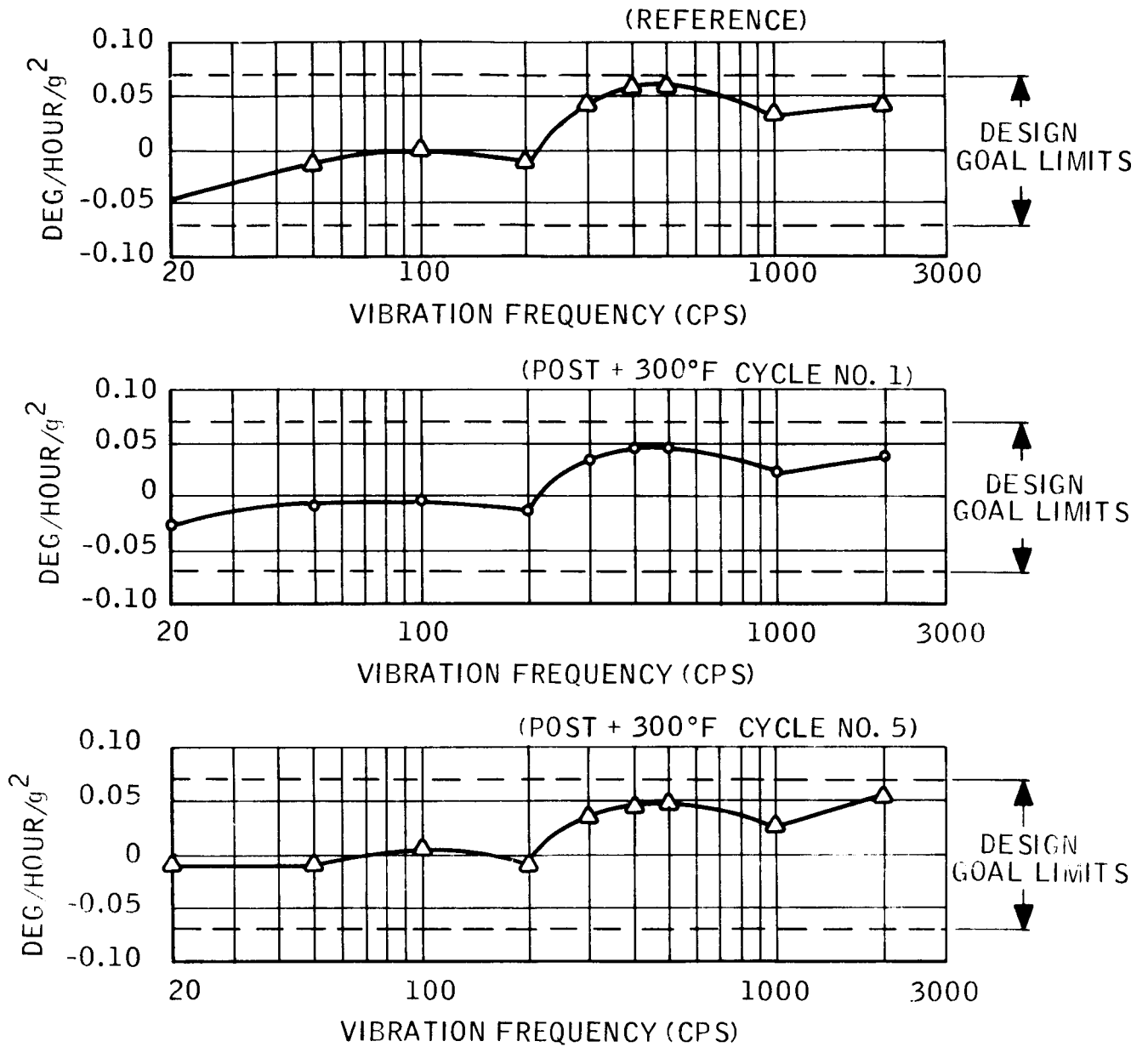


Figure 17. DGG159D1 Anisoelectric Drift Coefficients

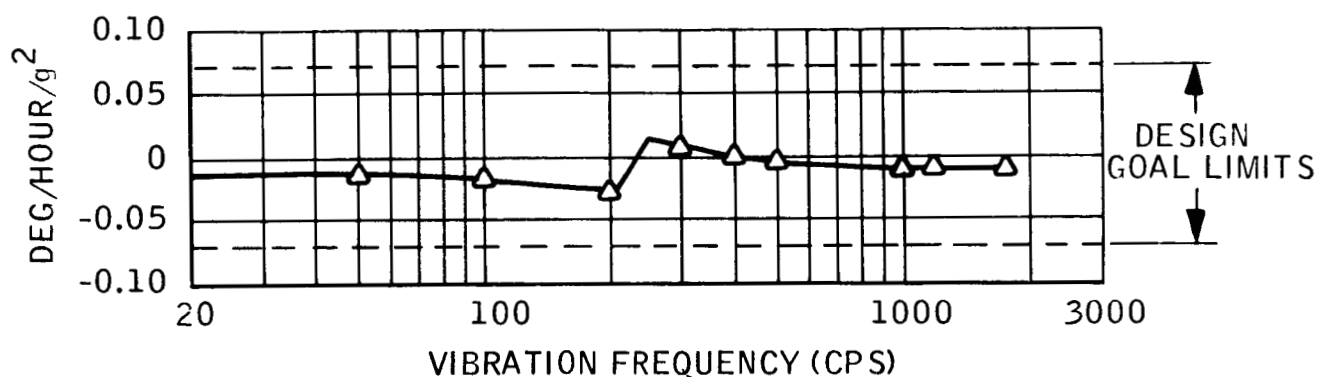


Figure 18. DGG159D Gyro Attitude Angle Drift Coefficient

#### Reference Drift Rate

The reference drift rate measured before the first sterilization cycle was:

g - insensitive	-0.38 deg/hr.
g - sensitive	
IA	+0.57 deg/hr.
SRA	+0.16 deg/hr.

#### Drift Rate Shift

The gyro drift rate was measured following each sterilization cycle after an eight-hour stabilization period. The sterilization drift rate shift is the difference in drift rate measured before and after the sterilization cycle.

Results are tabulated below:



Sterilization Drift Rate Shifts

	g-insensitive (° / Hr)	g-sensitive (° / Hr / g)	
		IA	SRA
Cycle 1	-0.26	+0.26	-0.34
Cycle 2	-0.07	-0.02	-0.09
Cycle 3	-0.07	-0.08	-0.07
Cycle 4	-0.09	-0.08	-0.10
Cycle 5	-0.04	-0.08	-0.13

Spinmotor Runup-to-Runup Stability

OA vertical runup-to-runup stability was measured following the reference drift rate measurement and after the first and fifth sterilization cycles. The drift rate given below is the value of five runups:

	OAV (deg/hr R.M.S)
Reference	0.011
Post 1st sterilization	0.007
Post 5th sterilization	0.000

Random Drift

Random drift measurements were made after the reference drift and after each sterilization cycle. The test period was four hours for the OAV, IA east and OAH, IA up orientations. Data points were 100-second integrated drift rate values. One sigma random drift values were:

	OAV (deg/hr)	IAV (deg/hr/g)
Reference	0.003	0.002
Post - 1st sterilization	0.003	0.002
Post - 2nd sterilization	0.001	0.001
Post - 3rd sterilization	0.001	0.002
Post - 4th sterilization	0.001	0.002
Post - 5th sterilization	0.002	0.003

The integrated drift rate points for the post - fifth sterilization cycle random drift run are tabulated in Tables 12 and 13. Actual magnitude of the drift rate is not indicated by the data points because of bias offset used to achieve the desired resolution.

### Gyro Parameters

Several other gyro parameters were measured in the course of the test program. These are listed below:

Signal generator sensitivity	23.7 mv/mr
Torquer scale factor	90.0 deg/hr/ma
Damping Coefficient	9,700 dcm-sec/rad
Gyro transfer function	234 volts/rad
Elastic restraint	0.038 deg/hr/mr
Gimbal freedom	+1.52 deg -1.51 deg
S.G. null voltage	1.5 mv

### Six-Position Test Results

G-sensitive and g-insensitive drift rates were determined throughout the test program from the six-position drift rate test. During this test the gyro was oriented in the following positions as established with a Leitz dividing head:

Table 12. OA Vertical Random Drift (Deg/Hr)

Data Point No.	Drift Rate	Data Point No.	Drift Rate	Data Point No.	Drift Rate	Data Point No.	Drift Rate
1	.4608	37	.4630	73	.4673	109	.4671
2	.4601	38	.4632	74	.4669	110	.4654
3	.4636	39	.4649	75	.4665	111	.4665
4	.4617	40	.4615	76	.4643	112	.4659
5	.4634	41	.4649	77	.4640	113	.4645
6	.4638	42	.4629	78	.4653	114	.4648
7	.4625	43	.4622	79	.4612	115	.4673
8	.4635	44	.4637	80	.4644	116	.4663
9	.4608	45	.4629	81	.4644	117	.4656
10	.4625	46	.4629	82	.4611	118	.4680
11	.4634	47	.4654	83	.4611	119	.4670
12	.4637	48	.4639	84	.4627	120	.4654
13	.4616	49	.4627	85	.4650	121	.4663
14	.4612	50	.4623	86	.4646	122	.4648
15	.4625	51	.4634	87	.4647	123	.4640
16	.4623	52	.4643	88	.4639	124	.4666
17	.4620	53	.4646	89	.4611	125	.4654
18	.4624	54	.4642	90	.4591	126	.4628
19	.4631	55	.4630	91	.4649	127	.4671
20	.4601	56	.4630	92	.4654	128	.4662
21	.4600	57	.4643	93	.4660	129	.4627
22	.4630	58	.4629	94	.4676	130	.4657
23	.4671	59	.4643	95	.4680	131	.4659
24	.4626	60	.4659	96	.4667	132	.4644
25	.4647	61	.4633	97	.4648	133	.4653
26	.4648	62	.4649	98	.4654	134	.4636
27	.4629	63	.4630	99	.4656	135	.4646
28	.4621	64	.4634	100	.4669	136	.4640
29	.4662	65	.4625	101	.4657	137	.4655
30	.4630	66	.4647	102	.4675	138	.4646
31	.4619	67	.4657	103	.4673	139	.4621
32	.4626	68	.4673	104	.4660	140	.4630
33	.4614	69	.4653	105	.4672	141	.4645
34	.4629	70	.4641	106	.4655	142	.4630
35	.4621	71	.4650	107	.4659	143	.4621
36	.4634	72	.4656	108	.4669	144	.4633

One Sigma = 0.002 °/Hr.

Table 13. IA Vertical Random Drift (Deg/Hr/g)

Data Point No.	Drift Rate	Data Point No.	Drift Rate	Data Point No.	Drift Rate	Data Point No.	Drift Rate
1	.4868	37	.4771	73	.4775	109	.4764
2	.4863	38	.4816	74	.4777	110	.4777
3	.4855	39	.4772	75	.4773	111	.4753
4	.4816	40	.4770	76	.4790	112	.4747
5	.4830	41	.4780	77	.4801	113	.4776
6	.4791	42	.4805	78	.4751	114	.4791
7	.4703	43	.4797	79	.4801	115	.4758
8	.4745	44	.4794	80	.4790	116	.4790
9	.4755	45	.4819	81	.4792	117	.4796
10	.4764	46	.4806	82	.4757	118	.4733
11	.4784	47	.4799	83	.4801	119	.4761
12	.4771	48	.4771	84	.4794	120	.4750
13	.4802	49	.4811	85	.4793	121	.4761
14	.4776	50	.4803	86	.4804	122	.4735
15	.4815	51	.4817	87	.4765	123	.4768
16	.4760	52	.4796	88	.4783	124	.4756
17	.4819	53	.4794	89	.4768	125	.4752
18	.4803	54	.4803	90	.4777	126	.4716
19	.4757	55	.4774	91	.4761	127	.4735
20	.4776	56	.4755	92	.4786	128	.4740
21	.4809	57	.4774	93	.4782	129	.4752
22	.4800	58	.4789	94	.4800	130	.4720
23	.4853	59	.4790	95	.4782	131	.4773
24	.4773	60	.4761	96	.4759	132	.4779
25	.4829	61	.4801	97	.4770	133	.4768
26	.4847	62	.4799	98	.4773	134	.4746
27	.4807	63	.4824	99	.4764	135	.4773
28	.4826	64	.4758	100	.4787	136	.4743
29	.4811	65	.4798	101	.4773	137	.4754
30	.4811	66	.4897	102	.4798	138	.4751
31	.4770	67	.4791	103	.4781	139	.4763
32	.4776	68	.4770	104	.4796	140	.4762
33	.4764	69	.4784	105	.4782	141	.4730
34	.4824	70	.4773	106	.4767	142	.4753
35	.4794	71	.4757	107	.4772	143	.4732
36	.4785	72	.4815	108	.4797	144	.4719

One Sigma = 0.003 °/Hr.

- (1) Output axis vertical down - Input axis East
- (2) Output axis vertical down - Input axis West
- (3) Output axis horizontal - Input axis up
- (4) Output axis horizontal - Input axis East
- (5) Output axis horizontal - Input axis down
- (6) Output axis horizontal - Input axis West

Drift rates were determined in each of the six positions by measuring the torque generator current in a closed rate servo loop. The drift rate measurements following the fifth sterilization cycle are tabulated below to illustrate the test method and the gyro repeatability.

Position	(1)	(2)	(3)	(4)	(5)	(6)
	-0.67	-0.68	+10.00	-0.93	-11.27	-0.39
	-0.67	-0.68	+10.00	-0.93	-11.27	-0.38

$$g - \text{insensitive} = \frac{(1) + (2)}{2} = -0.675 \text{ deg/hr.}$$

$$g - \text{sensitive IA} = \frac{(6) - (4)}{2} = +0.272 \text{ deg/hr/g.}$$

$$g - \text{sensitive SRA} = \frac{(5) - (3)}{2} + 10.64 = +0.005 \text{ deg/hr/g.}$$

Vertical Component of Earth's Rate at Minneapolis = 10.64 deg/hr/g.

The results of all six position tests on the DGG149D gyro throughout the test program are shown in Figure 19. The fluid torque drift is one component of the total g-insensitive drift, and is due to nonsymmetries of the hydrostatic gimbal support system. Fluid torque drift is the measured OAV drift change from pump-off to pump-on.

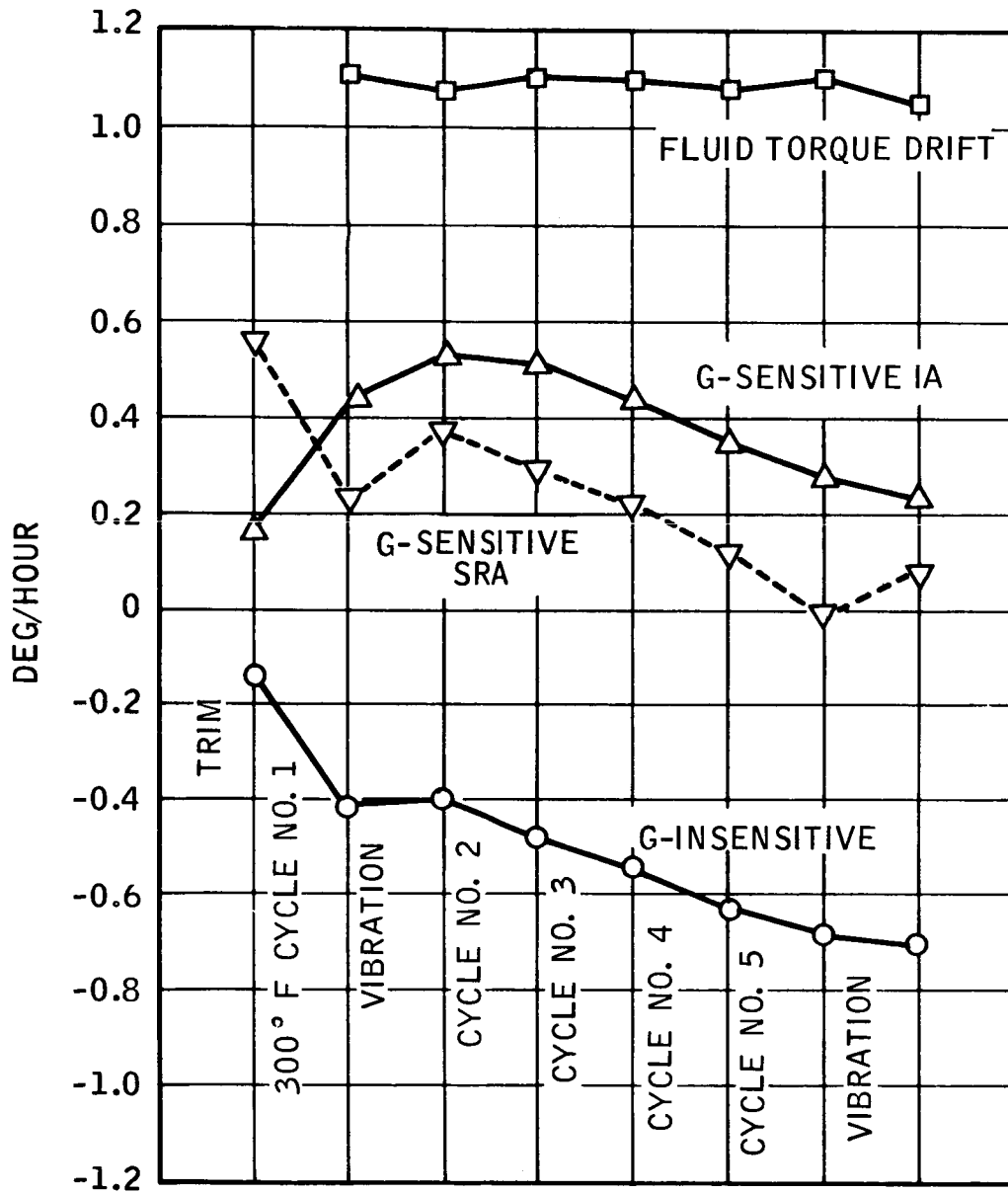


Figure 19. Gyro Drift History

## SPINMOTOR PERFORMANCE

An abnormal spinmotor condition was discovered on the DGG159D gyro after the final build and before initial calibration and adjustments. When the motor was turned off at operating temperature (185°F) it would not re-synchronize with up to 50 volts/phase of applied excitation. At room temperature the spinmotor would synchronize with 42 to 48 volts/phase and remain in sync when the voltage was reduced to 36 volts (normal excitation). This procedure was used during all of the final gyro performance testing.

### Starting Characteristics

The spinmotor starting voltages did not change appreciably during the five sterilization cycles. Minimum start voltages for the journal and thrust bearings are tabulated below:

	Journal	Thrust
Pre - sterilization	29.5 volts	36 volts
Post - 5th sterilization cycle	29 volts	37 volts

### Synchronous Characteristics

The spinmotor synchronous characteristics as a function of operating temperature were measured after gyro build, when the problem was discovered, and again after the five sterilization cycles were completed on the gyro. The synchronous speed characteristics are summarized in Table 14. In the temperature range from 130°F to 160°F the spinmotor speed is slightly less than synchronous with 48 v/φ applied; but when the voltage was rapidly decreased to 36 v/φ the motor would lock in at synchronous speed. Above 160°F it was not possible to bring the motor to synchronous speed.

Table 14. Synchronous Speed Characteristics

Temperature	Before Temperature Cycling		After 5 Sterilization Cycles	
	Sync Voltage	Method	Sync Voltage	Method
70° F	43-48	Normal	43-48	Normal
100° F	45-48	Normal	44-47	Normal
135° F		Runup at 48v, reduce quickly to 36v	--	Runup at 48v, reduce quickly to 36v

### Conclusions

The anisoelastic and attitude angle  $g^2$  drift of the GG159D met the performance goal of 0.07 deg/hr/ $g^2$  over the frequency range of 20 to 2000 cps. The anisoelastic drift term was generally stable within 0.01 deg/hr/ $g^2$  with sterilization cycling.

The performance goal of 0.10 deg/hr g-insensitive and 0.14 deg/hr g-sensitive drift stability over each sterilization cycle was met with exception of the first cycle. This, plus the trending of the drift terms shown in Figure 19, suggests that retrim will be necessary after one or more sterilization cycles to reduce the drift terms below 0.5 deg/hr. The trending of the drift terms appears to be reducing in rate, which could be verified by further testing.

The runup-to-runup stability and random drift of the DGG159D was well within the performance goals of 0.02 deg/hr RMS and 0.008 deg/hr (one sigma).



It is very difficult to draw a conclusion as to the abnormal spinmotor condition. Final data taken on the spinmotor and gimbal assembly, before the first gyro build, showed that the motor would synchronize at 185° F with 38 v/ø applied. The next spinmotor check following the second gyro build showed that the spinmotor would not synchronize with up to 50 v/ø applied. In between these two checks the following sequence of events occurred:

1. The gyro was built, filled and sealed.
2. Brief testing of the gyro was completed during which the gyro displayed poor (erratic) drift characteristics.
3. The gyro was machined open and disassembled.
4. The dielectric breakdown of the pump winding was discovered. A new pump assembly was fabricated.
5. The gyro was rebuilt, filled and sealed.
6. The gyro was placed on test and it was discovered that the spinmotor would not synchronize at 185° F.

This machining and rebuild sequence is normal processing for the GG159 gyro and ordinarily does not affect spinmotor performance in any way. Therefore, it must be concluded that the spinmotor was subjected to some unknown environment during the rebuild sequence which changed the synchronous torque margin.

## SECTION X RECOMMENDATIONS

### MAGNETIC

Study and development of the GG159 spinmotor magnetics should be accomplished to provide greater torque margin for the 36 volt/phase running condition. All productions of the GG159 spinmotors have used a 50-volt/phase start and synchronize, 26-volt/phase running excitation and the magnetics have been optimized for this condition. Further development in the following specific areas would provide additional torque margin for the starting and synchronizing of the spinmotor:

- Definition of Heat Treat Standards of the "H" ring for the 36-volt running condition
- Optimize the magnetic gap from stator to rotor.

### GYRO PERFORMANCE

Extensive long-term gyro testing should be accomplished to completely define gyro performance. The testing and data analysis should examine the following suspect areas:

- Flex lead material and configuration
- Stability of the g-insensitive drift trim magnets
- Effects of the coil cup on g-sensitive drift terms
- Relationship of nonsymmetrical gimbal areas, such of the gimbal fill plug, with the vector sum of g-sensitive drift changes.

The goal of this additional testing would be to determine if the drift rate trend noted during testing of the GG159D gyro is a long-term characteristic associated with repeated temperature cycling or of a short duration nature which would allow process stabilization. Specific areas requiring further development would be defined during the evaluation phase.

APPENDIX A  
GG159D GYRO TEST PROCEDURES

## APPENDIX A

### GG159D GYRO TEST PROCEDURES

Power supplying requirements for the DGG159D gyro are given in Table 14. The following procedures were used during performance testing.

#### GYRO DRIFT RATE READOUT

The gyro drift rate was determined by measuring the torque generator feedback current in a closed servo rate loop. The short term drift rates used to determine g-sensitive and g-insensitive drift values were recorded on a Brown-Honeywell recording millivoltmeter. The long term random drift rates were recorded on both the recording millivoltmeter and a Vidor voltage-to-frequency converter, preset counter and tape printer giving 100-second integrated drift rate values.

#### DIVIDER HEAD

All static gyro drift measurements were made with the gyro and holding fixture mounted on the face plate of a Leitz divider head.

#### GYRO HOLDING FIXTURES

- For all drift tests the gyro was mounted in an aluminum sleeve with a bakelite face plate.
- For vibration testing the gyro was mounted in an all-aluminum block with heating elements in the block.

## SIX-POSITION DRIFT RATE TEST

During this test short term drift rates were measured in the following gyro orientations as established with the Leitz divider head:

- Output axis vertical - Input axis; east, west
- Output axis horizontal - Input axis, up, down, east, west.

## STERILIZATION CYCLE

During the sterilization cycle the gyro was subjected to a 36-hour soak at 300° F, nonoperating followed by a cooldown to 50° F over a two-hour period.

## CALIBRATION AND ADJUSTMENTS

G-sensitive and g-insensitive drift rates were measured and adjusted, based on the six-position closed loop drift rate test.

## REFERENCE DRIFT RATE

Reference values of g-sensitive and g-insensitive drift before sterilization cycling were measured with the six-position test. The gyro was stabilized at operating temperature (185° F) for a minimum of four hours before beginning the test.

## STERILIZATION DRIFT RATE SHIFT

Six-position drift rate measurements were made after an eight-hour stabilization period at operating temperature following each sterilization cycle. The drift rate shift was the change in drift rate over the sterilization cycle.

## SPINMOTOR RUNUP-TO-RUNUP STABILITY

Runup-to-runup tests were made at operating temperature with the gyro oriented OAV and the IA rotated from east so that earth's rate balanced out the g-insensitive drift rate (null east). The test sequence was:

- a) measure short term drift rate
- b) turn off the spinmotor and allow it to completely run down to a stop
- c) excite the spinmotor and stabilize for five minutes at synchronous speed
- d) repeat (a), (b), and (c) four times for a total of five drift rate readings.

The runup-to-runup stability is the R.M.S. value of the five drift rate readings.

## RANDOM DRIFT

Random drift tests were made with the gyro oriented OAV, IA east and OAH, IA up. The gyro was stabilized at operating temperature for four hours followed by a four-hour random drift test. Data was 100 second integrated drift rate values from which one sigma values were calculated.

## $G^2$ DRIFT COEFFICIENTS

With the gyro fully operating and stabilized at operating temperature a sine wave vibration of 5 g's r.m.s. was applied during a five-minute frequency sweep from 20 to 2000 cps. The vibration was applied as follows:

- (a) Anisoelastic vibration was applied perpendicular to the OA and 45 degrees between the IA and SRA
- (b) Attitude angle vibration was applied in the OA-SRA plane 45 degrees between the OA and SRA.

The  $g^2$  drift coefficients were determined by dividing the change in drift rate at a given frequency by  $g^2$  which in this case was 25.

#### FLUID TORQUE DRIFT

Fluid torque drift was measured with the OAV, IA east. The hydrostatic pump was turned off and fluid torque drift was the measured change in drift rate from the pump on to pump off condition.

#### FLEX LEAD DRIFT RATE

Flex lead drift rate was calculated as the total g-insensitive drift minus fluid torque drift.